Journal of Solid Mechanics Vol. 14, No. 2 (2022) pp. 190-211
DOI: 10.22034/jsm.2021.1921133.1673

Analytical Solutions of Finite Wedges Coated by an Orthotropic Coating Containing Multiple Cracks and Cavities

A. Ajdari *

Department of Mechanical Engineering, Iran University of Science & Technology (IUST), Tehran, Iran

Received 18 February 2022; accepted 10 April 2022

ABSTRACT

This paper presents a general formulation for an isotropic wedge reinforced by an orthotropic coating involving multiple arbitrarily oriented defects under out of plane deformation. The exact closed form solution of the problem weakened by a screw dislocation in the isotropic wedge is obtained by making use of finite Fourier cosine transform. Also, the closed-form solutions of the out of plane stress and displacement fields are obtained. After that, by making use of a distributed dislocation approach, a set of singular integral equations of the domain involving smooth cavities and cracks subjected to out of plane external loading are achieved. The cracks and cavities are considered to be only in the isotropic wedge. The presented integral equations have Cauchy singularity and must be evaluated numerically. Multiple numerical examples will be presented to show the applicability and efficiency of the presented solution. The geometric and point load singularities of the stress components are obtained and compared with the available data in the literature.

Keywords : Out of plane; Isotropic wedges; Orthotropic coating; Mode III stress intensity factor; Hoop stress; Distributed dislocation method.

1 INTRODUCTION

WEDGES are often subjected to various loadings in the process of working. In the study of the fracture mechanics of Wedges, the structure of the coating seems to play an important role in a problem with multiple cracks. One important challenge in material design is reduction of the stress intensity factor in the cracked bars. To overcome this drawback, an efficient method is to introduce an effective coating layer. Coating is often applied to the surfaces of polymeric, metallic or composite structures. Coating layers are used for many reasons such as protecting, decorating, serving as a barrier, or providing unique surface properties. An appropriate coating can improve efficiency, component durability and fuel economy. In this paper, we use an orthotropic coating layer for reducing the stress intensity factor. The orthotropic materials, with properties that differ along three mutually-

*Corresponding author. Tel.: +98 21 7749 1232; Fax.: +98 21 7724 0406.
E-mail address: amirajdari68@gmail.com (A. Ajdari)

orthogonal twofold axes of rotational symmetry, are increasingly used as a coating of conventional materials in aerospace engineering as well as automobile and ship vehicles. This can be attributed to their high strength/density and stiffness/density ratios, high resistance to wear and heat penetration, low coefficient of friction and relatively low cost. On the other hand, the use of orthotropic materials as a coating for isotropic materials may be suggested for structural purposes, such as the reduction of stress intensity factors at the crack tips. In composite bodies, there are regions with high-stress levels due to cracks. These regions are the main reasons of failure in structures, even subjected to moderate loading. As the main step for designing a structure, the fracture analysis should be evaluated. Theoretical approaches are critical in fracture analysis for two important reasons. First, theoretical approaches exhibit the type of singularities that is employed to interpret experimental results and also to increase the correctness of numerical solutions. Second, theoretical approaches can provide general solutions for simple crack orientations and geometries and for specific material behavior that can be employed as a standard analysis for numerical evaluations [1]. Therefore, the fracture analysis of planes with simple geometries, including four-sided, wedges and circle is significant for the investigators in the fracture mechanic. For the out of plane fracture problems, dislocation approaches in solving a crack problem are well known, because a dislocation problem is a Green solution of the fracture problems [2]. There are not numerous papers focused on the out of plane problems of finite domains with coating weakened by cracks, like the paper of Matbuly et. al [3]. They were focused on the stress analysis of two cracks situated between the interface of two orthotropic four-sided domains under out of plane load. By making use of the finite Cosine Fourier transform, the solution was simplified to a group of Cauchy type integral equations, which had been evaluated numerically to obtain the stress intensity factor at crack tips. The paper was reexamined for further development by Li et. al [4] by making use of one interfacial crack.The analysis of wedge domains has been studied by multiple researchers. We first review the papers which have analyzed intact wedges. The problem of out of plane deformation of isotropic and dissimilar wedges subjected to anti-plane point load on straight borders was studied by Kargarnovin et. al [5] and Kargarnovin [6]. Similarly, the solution of an anisotropic wedge under out of plane deformation was the title of the paper done by Shahani [7]. In the next study, by making use of the aforementioned stress components and changing the angle of the sector, a circular domain weakened by one edge crack was analyzed. Recently, the stress intensity factor of double cantilever bars was derived by Shahani [8]. Stress analysis of dissimilar wedges subjected to out of plane point loads and weakened by a Voltra type screw dislocation by making use of the Mellin integral transform were presented by Lin et. al [9]. The wedges with equal angles had been connected to each other along the interface. They employed the Peach Koehler equation to obtain the stress components of the image loads applied on Voltra type dislocations. In next article, the stress analysis of an isotropic wedge under out of plane deformation was studied by Chen [10]. The boundary conditions consist of traction free and fixed conditions were assumed on straight borders of the wedge. The Laplace and Mellin transforms were employed to evaluate the problems. The author calculated the stress concentration factor of the wedge for various boundary conditions of the problem. Now, the earlier papers on wedges containing several cracks are reviewed. The out of plane solution of wedges weakened by some collinear cracks bisecting the angle of the wedges was presented by Mkhitaryan [11]. They employed the Mellin transform and the numerical solutions of Cauchy type integral equations to find the solution of the ensuring boundary problem and the stress intensity factors on crack tips. Shahani et.al [12] achieved the out of plane solution of an anisotropic sector containing a radial crack. The authors obtained the equilibrium equation with regard to complex functions with the aid of the suitable complex variables (see [13] for more details). The solution was simplified by making use of some integral transforms [7], which were similar to the typical Mellin transforms. Then, they calculated the stress intensity factor of the crack tips with the aid of a numerical evaluation of resultant integral equations.The out of plane analysis of infinite isotropic wedges involving several cracks was done by Faal [14]. The author derived the stress components of an intact wedge subjected to the point load on the isotropic wedge borders by making use of the Mellin integral transform. The Mellin integral transform and an imaginative approach were used by Faal et al. [15] to evaluate the out of plane deformation of finite wedges involving several elliptical cavities. Also, they obtained the stress components of intact finite wedge subjected to point loads on the borders. Among the numerical techniques, the finite element method is an important means to analyze the crack problems. In finite element analysis, it is conventional to model the crack tip singularity by using elements in which midside nodes are moved to quarter points. There is a widely used method of calculating of stress intensity factors which substitute the displacements, or the stresses, obtained from the finite element calculations, into standard field equations in the vicinity of crack tips. (For example, see [16]). One of the reasons of considering this reference here is the concept of Volterra distorsioni introduced there which is another feature of dislocation distribution technique. Pook, considered a pair of infinitesimal elements which are situated on the upper and lower surface of an unloaded crack respectively. These elements are connected by a ring element of infinitesimal width having a square cross section and located around the crack tip. He introduced the three of modes of dislocations of the six Volterra distorsioni (distortions), correspond to the three modes of crack tip surface

displacement. The remaining three Volterra distorsioni involve rotation of the above-mentioned elements which are usually called three modes of disclinations. He explained that the modes of crack surface displacements are a combination of some modes of dislocation and disclinations. In fact, the six Volterra distorsioni are useful in the description of crack displacements under load, and may also be used to describe narrow notch surface displacements as a model of crack. An interesting matter mentioned in this reference and also [17] which may be the main reason of considering these references here is about that different modes of displacements cannot exist in isolation. It can be seen in some applications such as, a cracked square plate and a cracked long bar in Mode III loading, but it is only for a special positions of the cracks.

From the literature survey, it appears that no publication has been devoted to study the effect of an orthotropic coating on the stress intensity factor in an isotropic finite wedge, even for a single crack. On the other hand, the most significant objective of the present study is to calculate the stress intensity factors of multiple cracks and cavities with arbitrary patterns by making use of the distributed dislocation technique. This dislocation arc is considered to be parallel with the interface of the isotropic wedge and its coating. The outline of this paper is as follows. The stress solution of an isotropic wedge with an orthotropic coating containing a screw dislocation is achieved in Section 2. For the sake of simplicity, the dislocation circular arc instead of a dislocation line is employed to describe the dislocation line. In section 3, the stress field of an isotropic wedge with an orthotropic coating under patch and point loads is found for the specific boundary conditions where the loads are applied on edges of the isotropic wedge. After that, Buckner's principle is employed to analyze the domain involving multiple smooth defects by making use of Sections 2 and 3. This method is presented in Section 4. In section 4, the dislocation approach is used to find Cauchy type singular integral equations. Next a group of algebraic equations for the calculation of stress intensity factors and hoop stresses around cavities are obtained with regard to the dislocation density function. In Section 5 the numerical examples are conducted to check the correctness of the present solutions. Furthermore, the effect of the orthotropic coating layer and crack parameters on the stress intensity factors is discussed in detail. Finally, concluding remarks are drawn in Section 6.

2 FORMULATION OF PROBLEM

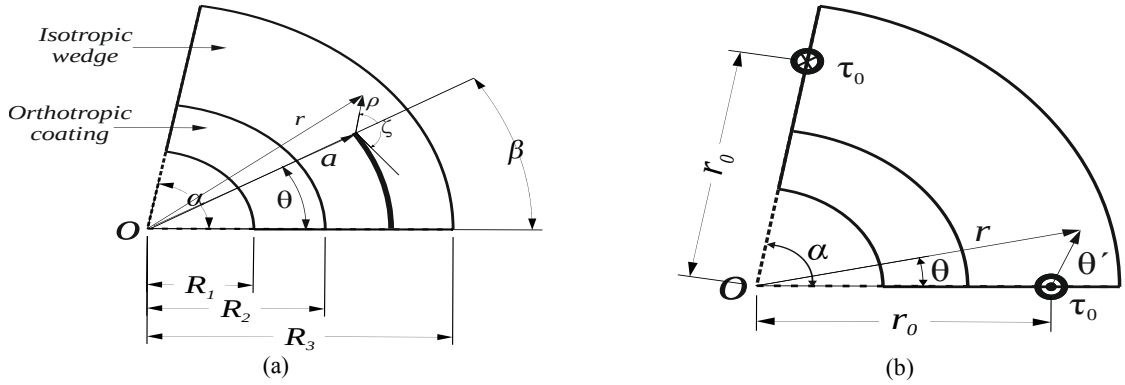

Fig.1
An isotropic wedge with an orthotropic coating subjected to out of plane loading.

The distributed dislocation technique is an efficient means of treating multiple curved cracks with smooth geometries. However, determining stress fields due to a single dislocation in the region has been a major obstacle to the utilization of this method. In fracture analysis, a so-called 'dislocation method' is frequently used in analyzing smooth defects [2]. This approach depends on the stress components corresponding to a dislocation path in the domain under consideration. For an isotropic wedge with an orthotropic coating wedge weakened by a Volterra type screw dislocation, this approach is developed subjected to out of plane loading. The configuration of the isotropic wedge and its orthotropic coating is observed in Fig.1(a), in which R_2 and R_3 are the inner and outer radius of the isotropic substrate. The wedge angle of the entire domain is considered to be α and the orthotropic coating thickness is $R_2 - R_1$. The origin of the cylindrical coordinate system is set at the center of non-straight borders of the domain and the angle of the cylindrical coordinate system is measured from the lower border of the domain under consideration. The coating of the isotropic substrate is made of orthotropic material, in which G_{rz} and $G_{\theta z}$

are the shear modulus in r and θ directions. A Volterra type screw dislocation with Burgers vector b_z is considered at the location (a,β) of the isotropic wedge shear moduli μ_0 with the dislocation arc $r=a$. The dislocation circular arc instead of a dislocation straight line is offered in this paper (see [14, 15, 23, 24]). Then, the domain under consideration divided into three sub-domains $R_1 \le r \le R_2$ (region 1), $R_2 \le r \le a$ (region 2) and $a \le r \le R_3$ (region 3). The circular borders of the domain under consideration at $r=R_1$ and $r=R_2$ are considered to be clamped. The only non-zero displacement component subjected to out of plane loading is the displacement $w(r,\theta)$ in each sub-region. The non-vanishing displacement component under out of plane deformation is the displacement component $w(r,\theta)$ in each sub-domain. The equation of equilibrium in the lack of external forces and moments in the cylindrical coordinate system is stated as:

$$\frac{\partial \tau_{rz}}{\partial r}+\frac{1}{r}\frac{\partial \tau_{\theta z}}{\partial \theta}+\frac{\tau_{rz}}{r}=0 \tag{1}$$

The non-zero stress components of the problem by making use of the constitutive equations for are written as:

$$\begin{aligned}&\tau_{rz}=G_{rz}\frac{\partial w}{\partial r}\ ,R_1\le r\le R_2\ ,\ \tau_{\theta z}=G_{\theta z}\frac{1}{r}\frac{\partial w}{\partial \theta}\ ,R_1\le r\le R_2\\&\tau_{rz}=\mu_0\frac{\partial w}{\partial r}\ ,R_2\le r\le R_3\ ,\ \tau_{\theta z}=\mu_0\frac{1}{r}\frac{\partial w}{\partial \theta}\ ,\ R_2\le r\le R_3\end{aligned} \tag{2}$$

By substitution of Eq. (2) into Eq. (1) the governing equation of the orthotropic coating is found as:

$$r^2\frac{\partial^2 w}{\partial r^2}+r\frac{\partial w}{\partial r}+G^2\frac{\partial^2 w}{\partial \theta^2}=0 \tag{3}$$

In which $G=\sqrt{G_{\theta z}/G_{rz}}$ denotes the orthotropic ratio. The governing equation of the isotropic substrate is easily found by setting $G=1$ in Eq. (3). Consider the following Fourier transform and whose inversion as:

$$G(n)=\int_0^{\alpha} g(\theta)\cos\frac{n\pi\theta}{\alpha}d\theta\ ,\qquad g(\theta)=\frac{2}{\alpha}\sum_{n=1}^{\infty}G(n)\cos\frac{n\pi\theta}{\alpha} \tag{4}$$

The stress-free conditions on the wedge straight borders and the clamped conditions on the circular edges yield

$$\begin{aligned}&\frac{\partial w(r,0)}{\partial \theta}=0,\quad \frac{\partial w(r,\alpha)}{\partial \theta}=0\\&w(R_1,\theta)=0,\quad w(R_3,\theta)=0\end{aligned} \tag{5}$$

By making use of Fourier transform (4) and the conditions (5) the partial differential Eq. (3) is written as:

$$r^2\frac{\partial^2 W(r,n)}{\partial r^2}+r\frac{\partial W(r,n)}{\partial r}-(n\kappa)^2 W(r,n)=0 \tag{6}$$

In which $\kappa=\frac{G\pi}{\alpha}$ and $W(r,n)$ is the Fourier transform of $w(r,\theta)$. The solution of Eq. (6) is found as follows:

$$W(r,n)=A_{kn}r^{Gn\kappa}+B_{kn}r^{-Gn\kappa},k=1,2,3 \tag{7}$$

In which the unknown constants will be obtained with the aid of the appropriate continuity and boundary conditions. The Subscript k refers to the sub-domains $R_1 \le r \le R_2$, $R_2 \le r \le a$ and $a \le r \le R_2$, in which a is the radius of the dislocation circular arc. With the aid of Eq. (7), the anti-plane displacement $w\left(r,\theta\right)$ is found as follows:

$$w\left(r,\theta\right)=\frac{2}{\alpha}\sum_{n=1}^{\infty}\left(A_{kn}r^{Gn\kappa}+B_{kn}r^{-Gn\kappa}\right)cos\,\frac{n\pi\theta}{\alpha},k=1,2,3 \tag{8}$$

The boundary condition corresponding to the screw dislocation under out of plane loading is defined as:

$$w\left(a^{-},\theta\right)-w\left(a^{+},\theta\right)=\delta H\left(\beta-\theta\right) \tag{9}$$

In which H refers to the unit step function. The self-equilibrium of the stress component in the wedge weakened by the screw dislocation is written as:

$$\tau_{rz}\left(a^{+},\theta\right)=\tau_{rz}\left(a^{-},\theta\right) \tag{10}$$

Continuity of stress and displacements between the isotropic wedge and its coating can be expressed as:

$$w\left(R_2^{+},\theta\right)=w\left(R_2^{-},\theta\right),\ \ \tau_{rz}\left(R_2^{+},\theta\right)=\tau_{rz}\left(R_2^{-},\theta\right) \tag{11}$$

By applying the finite Fourier transform to Eq. (9) and considering Eq. (11), we have

$$\begin{aligned}&W\left(a^{-},n\right)-W\left(a^{+},n\right)=(\delta\alpha/n\pi)\sin(n\pi\beta/\alpha)\\&\frac{\partial W\left(a^{+},n\right)}{\partial r}-\frac{\partial W\left(a^{-},n\right)}{\partial r}=0,\ W\left(R_2^{+},n\right)=W\left(R_2^{-},n\right),\ \frac{\partial}{\partial r}W\left(R_2^{+},n\right)-G\,\frac{\partial}{\partial r}W\left(R_2^{-},n\right)=0\end{aligned} \tag{12}$$

In which $\bar{\mu}=\mu_0/G_{rz}$. It can be realized that the first pair of conditions (5) is automatically satisfied. By applying the continuity conditions (12) and the second pair of conditions (5) to Eq. (7) we have

$$\begin{aligned}&A_{1n}R_1^{\,n\kappa}+B_{1n}R_1^{\,-n\kappa}=0,\quad A_{3n}R_3^{\,Gn\kappa}+B_{3n}R_3^{\,-Gn\kappa}=0\\&A_{1n}R_2^{\,n\kappa}+B_{1n}R_2^{\,-n\kappa}-A_{2n}R_2^{\,Gn\kappa}-B_{2n}R_2^{\,-Gn\kappa}=0,\ A_{1n}R_2^{\,n\kappa}-B_{1n}R_2^{\,-n\kappa}-\bar{\mu}A_{2n}R_2^{\,n\kappa}+\bar{\mu}B_{2n}R_2^{\,-n\kappa}=0\\&A_{3n}a^{Gn\kappa}+B_{3n}a^{-Gn\kappa}-A_{2n}a^{Gn\kappa}-B_{2n}a^{-Gn\kappa}=\frac{\delta\alpha}{n\pi}\sin n\kappa\beta\\&A_{3n}a^{Gn\kappa}-B_{3n}a^{-Gn\kappa}-A_{2n}a^{Gn\kappa}-B_{2n}a^{-Gn\kappa}=0\end{aligned} \tag{13}$$

Solving the algebraic Eq. (13) yields

$$\begin{aligned}&A_{1n}=\Lambda_{\mathrm{n}}\left(-1-\left(a/R_3\right)^{2n\kappa}\right)(b_z\alpha/\pi)\bar{\mu}a^{-n\kappa},\qquad B_{1n}=\Lambda_{\mathrm{n}}\left(1+\left(a/R_3\right)^{2n\kappa}\right)(b_z\alpha/\pi)\bar{\mu}(R_1^2/a)^{n\kappa}\\&A_{2n}=\Lambda_{\mathrm{n}}\left(-\left(\bar{\mu}+1\right)+\left(R_1/R_2\right)^{2Gn\kappa}\left(\bar{\mu}-1\right)\right)\left(1+\left(a/R_3\right)^{2Gn\kappa}\right)(b_z\alpha/\pi)a^{-Gn\kappa}\\&B_{2n}=\Lambda_{\mathrm{n}}\left(-\left(R_1/R_2\right)^{2Gn\kappa}\left(G+1\right)+\left(G-1\right)\right)\left(-1-\left(a/R_3\right)^{2Gn\kappa}\right)(b_z\alpha/2\pi)\left(R_2^2/a\right)^{Gn\kappa}\\&A_{3n}=-\Lambda_{\mathrm{n}}\left(-\left(R_2/a\right)^{2Gn\kappa}+\left(G-1\right)\left(R_1/R_2\right)^{2Gn\kappa}-\left(\bar{\mu}+1\right)\left(1+\left(R_1/a\right)^{2Gn\kappa}\right)\right)(b_z\alpha/2\pi)\left(a/R_3^2\right)^{n\kappa}\\&B_{3n}=-\Lambda_{\mathrm{n}}\left(-\left(G-1\right)\left(R_1/R_2\right)^{2Gn\kappa}+\left(R_2/a\right)^{2Gn\kappa}+\left(\bar{\mu}+1\right)\left(1+\left(R_1/a\right)^{2Gn\kappa}\right)\right)(b_z\alpha/2\pi)\left(a/R_3^2\right)^{n\kappa}\end{aligned} \tag{14}$$

In which $\Lambda_{\mathrm{n}}=\dfrac{\sin\left(n\pi\beta/\alpha\right)}{n\left(\left(\bar{\mu}+1\right)\left(-(R_1/R_2)^{2n\kappa}+(R_2/R_3)^{2Gn\kappa}\right)+\left(\bar{\mu}+1\right)\left(-(R_1/R_3)^{2Gn\kappa}+1\right)\right)}$. Upon substitution of the coefficients (14) into Eq. (8) the displacement field of the problem yields

$$
\begin{aligned}
w\left(r,\theta\right)&=\frac{2b_z\,\bar{\mu}}{\pi}\sum_{n=1}^{\infty}\Lambda_{\mathrm{n}}\left(-\left(r/a\right)^{n\kappa}-\left(ar/R_3^{\,2}\right)^{n\kappa}+\left(aR_1^{\,2}/rR_3^{\,2}\right)^{n\kappa}+\left(R_1^{\,2}/ra\right)^{n\kappa}\right)\cos n\kappa\theta,\qquad R_1\le r\le R_2\\
w\left(r,\theta\right)&=\frac{b_z}{\pi}\sum_{n=1}^{\infty}\Lambda_{\mathrm{n}}\left(\left(\bar{\mu}+1\right)(-\left(ra/R_3^{\,2}\right)^{Gn\kappa}+\left(aR_1^{\,2}/rR_3^{\,2}\right)^{Gn\kappa}-\left(r/a\right)^{Gn\kappa}+\left(R_1^{\,2}/ra\right)^{Gn\kappa})\right.\\
&\left.-\left(\bar{\mu}-1\right)(-\left(raR_1^{\,2}/R_2^{\,2}R_3^{\,2}\right)^{Gn\kappa}+\left(aR_1^{\,2}/rR_3^{\,2}\right)^{Gn\kappa}-\left(rR_1^{\,2}/aR_2^{\,2}\right)^{Gn\kappa}+\left(R_2^{\,2}/ra\right)^{Gn\kappa}))\cos n\kappa\theta,\qquad R_2\le r\le a\right.\\
w\left(r,\theta\right)&=-\frac{b_z}{\pi}\sum_{n=1}^{\infty}\Lambda_{\mathrm{n}}\left(\left(\bar{\mu}+1\right)(\left(ra/R_3^{\,2}\right)^{Gn\kappa}+\left(rR_1^{\,2}/aR_3^{\,2}\right)^{Gn\kappa}-\left(a/r\right)^{Gn\kappa}-\left(R_1^{\,2}/ra\right)^{Gn\kappa})\right.\\
&\left.-\left(\bar{\mu}-1\right)(+\left(raR_1^{\,2}/R_2^{\,2}R_3^{\,2}\right)^{Gn\kappa}+\left(rR_2^{\,2}/aR_3^{\,2}\right)^{Gn\kappa}-\left(aR_1^{\,2}/rR_2^{\,2}\right)^{Gn\kappa}-\left(R_2^{\,2}/ra\right)^{Gn\kappa}))\cos n\kappa\theta,\qquad a\le r\le R_3\right.
\end{aligned}
\tag{15}
$$

Substituting Eq. (15) into Eq. (2), the stress components is derived as follows:

$$
\begin{aligned}
\tau_{\theta z}\left(r,\theta\right)&=-\frac{2b_zG_{\theta z}}{r\alpha}\sum_{n=1}^{\infty}n\Lambda_{\mathrm{n}}\left(-\left(ar/R_3^{\,2}\right)^{n\kappa}+\left(aR_1^{\,2}/rR_3^{\,2}\right)^{n\kappa}-\left(r/a\right)^{n\kappa}+\left(R_1^{\,2}/ra\right)^{n\kappa}\right)\sin n\kappa\theta,\quad R_1\le r\le R_2\\
\tau_{\theta z}\left(r,\theta\right)&=-\frac{b_zG_{\theta z}}{r\alpha}\sum_{n=1}^{\infty}n\Lambda_{\mathrm{n}}\left(\left(\bar{\mu}+1\right)(-\left(ra/R_3^{\,2}\right)^{Gn\kappa}+\left(aR_1^{\,2}/rR_3^{\,2}\right)^{Gn\kappa}-\left(r/a\right)^{Gn\kappa}+\left(R_1^{\,2}/ra\right)^{Gn\kappa})\right.\\
&\left.-\left(\bar{\mu}-1\right)(-\left(raR_1^{\,2}/R_2^{\,2}R_3^{\,2}\right)^{Gn\kappa}+\left(aR_1^{\,2}/rR_3^{\,2}\right)^{Gn\kappa}-\left(rR_1^{\,2}/aR_2^{\,2}\right)^{Gn\kappa}+\left(R_2^{\,2}/ra\right)^{Gn\kappa}))\sin n\kappa\theta,\qquad R_2\le r\le a\right.\\
\tau_{\theta z}\left(r,\theta\right)&=\frac{b_zG_{\theta z}}{r\alpha}\sum_{n=1}^{\infty}n\Lambda_{\mathrm{n}}\left(\left(\bar{\mu}+1\right)(+\left(ra/R_3^{\,2}\right)^{Gn\kappa}+\left(rR_1^{\,2}/aR_3^{\,2}\right)^{Gn\kappa}-\left(a/r\right)^{Gn\kappa}-\left(R_1^{\,2}/ra\right)^{Gn\kappa})\right.\\
&\left.-\left(\bar{\mu}-1\right)(+\left(raR_1^{\,2}/R_2^{\,2}R_3^{\,2}\right)^{Gn\kappa}+\left(rR_2^{\,2}/aR_3^{\,2}\right)^{Gn\kappa}-\left(aR_1^{\,2}/rR_2^{\,2}\right)^{Gn\kappa}-\left(R_2^{\,2}/ra\right)^{Gn\kappa}))\sin n\kappa\theta,\qquad a\le r\le R_3\right.\\
\tau_{rz}\left(r,\theta\right)&=\frac{2b_z\,\mu_0\bar{\mu}}{r\alpha}\sum_{n=1}^{\infty}n\Lambda_{\mathrm{n}}\left(+\left(ar/R_3^{\,2}\right)^{n\kappa}+\left(aR_1^{\,2}/rR_3^{\,2}\right)^{n\kappa}+\left(r/a\right)^{n\kappa}+\left(R_1^{\,2}/ra\right)^{n\kappa}\right)\cos n\kappa\theta,\qquad R_1\le r\le R_2\\
\tau_{rz}\left(r,\theta\right)&=-\frac{b_zG_{rz}}{r\alpha}\sum_{n=1}^{\infty}n\Lambda_{\mathrm{n}}\left(\left(\bar{\mu}+1\right)(\left(ra/R_3^{\,2}\right)^{Gn\kappa}+\left(aR_1^{\,2}/rR_3^{\,2}\right)^{Gn\kappa}+\left(r/a\right)^{Gn\kappa}+\left(R_1^{\,2}/ra\right)^{Gn\kappa})\right.\\
&\left.-\left(\bar{\mu}-1\right)(\left(raR_1^{\,2}/R_2^{\,2}R_3^{\,2}\right)^{Gn\kappa}+\left(aR_1^{\,2}/rR_3^{\,2}\right)^{Gn\kappa}+\left(rR_1^{\,2}/aR_2^{\,2}\right)^{Gn\kappa}+\left(R_2^{\,2}/ra\right)^{Gn\kappa}))\cos n\kappa\theta,\qquad R_2\le r\le a\right.\\
\tau_{rz}\left(r,\theta\right)&=-\frac{b_zG_{rz}}{r\alpha}\sum_{n=1}^{\infty}\Lambda_{\mathrm{n}}\left(\left(\bar{\mu}+1\right)(\left(ra/R_3^{\,2}\right)^{Gn\kappa}+\left(rR_1^{\,2}/aR_3^{\,2}\right)^{Gn\kappa}+\left(R_1^{\,2}/ra\right)^{Gn\kappa}+\left(a/r\right)^{Gn\kappa})\right.\\
&\left.-\left(\bar{\mu}-1\right)(\left(raR_1^{\,2}/R_2^{\,2}R_3^{\,2}\right)^{Gn\kappa}+\left(rR_2^{\,2}/aR_3^{\,2}\right)^{Gn\kappa}+\left(aR_1^{\,2}/rR_2^{\,2}\right)^{Gn\kappa}+\left(R_2^{\,2}/ra\right)^{Gn\kappa}))\cos n\kappa\theta,\qquad a\le r\le R_3\right.
\end{aligned}
\tag{16}
$$

We can obtain the stress component $\tau_{rz}\left(r,\theta\right)$ in the sub-domain $a\le r\le R_3$ by changing r/a with a/r in the equation of $\tau_{rz}\left(r,\theta\right)$ for the sub-domain $R_2\le r\le a$. Similar changes help us find the stress component $\tau_{\theta z}\left(r,\theta\right)$ for each sub-domain. Furthermore, the changed items are multiplied by a minus sign. By making use of the expansion $n\Lambda_{\mathrm{n}}=\sin n\kappa\beta\sum_{m=0}^{\infty}\sum_{l=0}^{m}\sum_{d=0}^{\infty}\left(\left(\frac{R_2}{R_3}\right)^{2mG}\left(\frac{R_1R_3}{R_2^{\,2}}\right)^{2l}\left(\frac{R_1}{R_3}\right)^{2d}\right)^{n\kappa}(-1)^{m+1}\frac{(m+d)!}{l!\,d!\,(m-l)!}\frac{(\bar{\mu}-1)^m}{(\bar{\mu}+1)^{m+1}}$ (see reference [23]). After that, the stress field (16) is summed over the domain under consideration as:

$$\tau_{\theta z}\left(r,\theta\right)=\frac{b_z\,\mu_0\bar{\mu}}{2r\alpha}\sum_{m=0}^{\infty}\sum_{l=0}^{m}\sum_{d=0}^{\infty}\Omega_{ld}^{m}\{q_{ld}^{m}\left(\frac{ra}{R_3^2},\beta-\theta\right)+q_{ld}^{m}\left(\frac{r}{a},\beta-\theta\right)-q_{ld}^{m}\left(\frac{aR_1^2}{rR_3^2},\beta-\theta\right)-q_{ld}^{m}\left(\frac{R_1^2}{ra},\beta-\theta\right)$$
$$+q_{ld}^{m}\left(\frac{aR_1^2}{rR_3^2},\beta+\theta\right)-q_{ld}^{m}\left(\frac{ra}{R_3^2},\beta+\theta\right)+q_{ld}^{m}\left(\frac{R_1^2}{ra},\beta+\theta\right)-q_{ld}^{m}\left(\frac{r}{a},\beta+\theta\right)\},\quad R_1\le r\le R_2$$
$$\tau_{\theta z}\left(r,\theta\right)=\frac{b_z G_{\theta z}}{2r\alpha}\sum_{m=0}^{\infty}\sum_{l=0}^{m}\sum_{d=0}^{\infty}\Omega_{ld}^{m}\{(\bar{\mu}+1)[q_{ld}^{m}\left(\frac{ra}{R_3^2},\beta-\theta\right)-q_{ld}^{m}\left(\frac{R_1^2}{ra},\beta-\theta\right)+q_{ld}^{m}\left(\frac{ra}{R_3^2},\beta+\theta\right)$$
$$-q_{ld}^{m}\left(\frac{aR_1^2}{rR_3^2},\beta-\theta\right)+q_{ld}^{m}\left(\frac{r}{a},\beta+\theta\right)-q_{ld}^{m}\left(\frac{aR_1^2}{rR_3^2},\beta+\theta\right)+q_{ld}^{m}\left(\frac{r}{a},\beta-\theta\right)-q_{ld}^{m}\left(\frac{R_1^2}{ra},\beta+\theta\right)]-(G-1)$$
$$[-q_{ld}^{m}\left(\frac{raR_1^2}{R_2^2R_3^2},\beta+\theta\right)+q_{ld}^{m}\left(\frac{aR_1^2}{rR_3^2},\beta+\theta\right)-q_{ld}^{m}\left(\frac{rR_1^2}{aR_2^2},\beta-\theta\right)+q_{ld}^{m}\left(\frac{aR_1^2}{rR_3^2},\beta-\theta\right)+q_{ld}^{m}\left(\frac{R_2^2}{ra},\beta+\theta\right)$$
$$-q_{ld}^{m}\left(\frac{R_2^2}{ra},\beta-\theta\right)+q_{ld}^{m}\left(\frac{raR_1^2}{R_2^2R_3^2},\beta-\theta\right)+q_{ld}^{m}\left(\frac{rR_1^2}{aR_2^2},\beta-\theta\right)],\quad R_2\le r\le a$$
$$\tau_{rz}\left(r,\theta\right)=\frac{b_z\,\mu_0\bar{\mu}}{2r\alpha}\sum_{m=0}^{\infty}\sum_{l=0}^{m}\sum_{d=0}^{\infty}\Omega_{ld}^{m}\{p_{ld}^{m}\left(\frac{ra}{R_3^2},\beta-\theta\right)+p_{ld}^{m}\left(\frac{r}{a},\beta-\theta\right)+p_{ld}^{m}\left(\frac{aR_1^2}{rR_3^2},\beta-\theta\right)$$
$$+p_{ld}^{m}\left(\frac{ra}{R_3^2},\beta+\theta\right)+p_{ld}^{m}\left(\frac{R_1^2}{ra},\beta-\theta\right)+p_{ld}^{m}\left(\frac{aR_1^2}{rR_3^2},\beta+\theta\right)+p_{ld}^{m}\left(\frac{R_1^2}{ra},\beta+\theta\right)+p_{ld}^{m}\left(\frac{r}{a},\beta+\theta\right)\},\quad R_1\le r\le R_2$$
$$\tau_{rz}\left(r,\theta\right)=\frac{b_z G_{rz}}{4r\alpha}\sum_{m=0}^{\infty}\sum_{l=0}^{m}\sum_{d=0}^{\infty}\Omega_{ld}^{m}\{(\bar{\mu}+1)[p_{ld}^{m}\left(\frac{ra}{R_3^2},\beta-\theta\right)+p_{ld}^{m}\left(\frac{r}{a},\beta-\theta\right)+p_{ld}^{m}\left(\frac{aR_1^2}{rR_3^2},\beta-\theta\right)$$
$$+p_{ld}^{m}\left(\frac{R_1^2}{ra},\beta-\theta\right)+p_{ld}^{m}\left(\frac{aR_1^2}{rR_3^2},\beta+\theta\right)+p_{ld}^{m}\left(\frac{ra}{R_3^2},\beta+\theta\right)+p_{ld}^{m}\left(\frac{R_1^2}{ra},\beta+\theta\right)+p_{ld}^{m}\left(\frac{r}{a},\beta+\theta\right)]-(\bar{\mu}-1)$$
$$[p_{ld}^{m}\left(\frac{aR_1^2}{rR_3^2},\beta+\theta\right)+p_{ld}^{m}\left(\frac{R_2^2}{ra},\beta-\theta\right)+p_{ld}^{m}\left(\frac{raR_1^2}{R_2^2R_3^2},\beta+\theta\right)+p_{ld}^{m}\left(\frac{raR_1^2}{R_2^2R_3^2},\beta-\theta\right)$$
$$+p_{ld}^{m}\left(\frac{rR_1^2}{aR_2^2},\beta-\theta\right)+p_{ld}^{m}\left(R_2^2/ra,\beta-\theta\right)+p_{ld}^{m}\left(\frac{aR_1^2}{rR_3^2},\beta-\theta\right)+p_{ld}^{m}\left(\left(rR_1^2/aR_2^2\right)^{n\kappa},\beta-\theta\right)],\quad R_2\le r\le a \tag{17}$$

where $\Omega_{ld}^{m}=\frac{(m+d)!}{l!\,d!\,(m-l)!}\frac{(\bar{\mu}-1)^m}{(\bar{\mu}+1)^{m+1}}(-1)^{m+l+1}$ and

$$q_{ld}^{m}\left(x,\theta,\kappa,R_1,R_2,R_3\right)=\frac{\sinh(\kappa\ln\left(\left(\frac{R_1R_3}{R_2^2}\right)^{2l}\left(\frac{R_1}{R_3}\right)^{2d}\left(\frac{R_2}{R_3}\right)^{2Gm}x\right))}{\cosh(\kappa\ln\left(\left(\frac{R_1R_3}{R_2^2}\right)^{2l}\left(\frac{R_1}{R_3}\right)^{2d}\left(\frac{R_2}{R_3}\right)^{2Gm}x\right))-\cos\kappa\theta}$$
$$p_{ld}^{m}\left(x,\theta,\kappa,R_1,R_2,R_3\right)=\frac{\sin\kappa\theta}{\cosh(\kappa\ln\left(\left(\frac{R_1R_3}{R_2^2}\right)^{2l}\left(\frac{R_1}{R_3}\right)^{2d}\left(\frac{R_2}{R_3}\right)^{2Gm}x\right))-\cos\kappa\theta} \tag{18}$$

The constants κ, R_1, R_2 and R_3 have been removed from Eq. (17) for brevity. Two main reasons can be mentioned to rewrite stress filed (16) in the form of Eq. (17). First, the new defined functions

$q_{ld}^{m}\left(x,\theta,\kappa,R_1,R_2,R_3\right)$ and $p_{ld}^{m}\left(x,\theta,\kappa,R_1,R_2,R_3\right)$ can converge very fast for large values of m, l and d because of $l \le m$ and $\left(\frac{R_2}{R_3}\right)^m \left(\frac{R_1 R_3}{R_2^2}\right)^l \le \left(\frac{R_1}{R_3}\right)^m$. In addition, by setting $R_1 = 0$ and $\bar{\mu} = 1$ the newly defined functions are eliminated for all values of m, l and d and the stress filed of the finite wedge without coating is derived in term of $q_{00}^{0}\left(x,\theta,\kappa,0,R_2,R_3\right)$ and $p_{00}^{0}\left(x,\theta,\kappa,0,R_2,R_3\right)$. The comparison between ensuring stress components for $R_1 = 0$ and the results presented by Faal et al. [23] exhibits an excellent agreement. It is to be noted that the screw dislocation path in the aforementioned reference was a straight line but in the present study a circular arc is used to make the dislocation cut and despite the differences, the final result was the same. In the next step, the singularity of stress components at the dislocation point is investigated. So we use a local coordinate system as shown in Fig. 1(a). We can write the following relationships between the global and local coordinates as follows:

$$\theta = \beta - sin^{-1}\left(\frac{\rho cos\,\xi}{\sqrt{a^2+\rho^2+2a\rho sin\,\xi}}\right), r = \sqrt{a^2+\rho^2+2a\rho sin\,\xi}, 0 \le \xi \le 2\pi \tag{19}$$

Upon substituting Eq. (19) into the factions $q_{ld}^{m}\left(r/a,\beta-\theta,\kappa,R_1,R_2,R_3\right)$ and $p_{ld}^{m}\left(r/a,\beta-\theta,\kappa,R_1,R_2,R_3\right)$ and some mathematical operations we have

$$\begin{aligned} q_{00}^{0}\left(r/a,\beta-\theta,\kappa,R_1,R_2,R_3\right) &\sim \frac{\alpha sin\,\xi}{2\pi cos^2\xi}\frac{1}{\rho}, \text{ as } \rho \to 0, 0 \le \xi \le 2\pi \\ p_{00}^{0}\left(r/a,\beta-\theta,\kappa,R_1,R_2,R_3\right) &\sim \frac{2\alpha}{\pi cos\,\xi}\frac{1}{\rho}, \text{ as } \rho \to 0, 0 \le \xi \le 2\pi \end{aligned} \tag{20}$$

Due to the Eq. (20) we have $(\tau_{\theta z}, \tau_{rz}) \sim \frac{1}{\rho}$ as $\rho \to 0$. Weertman [25] has reported this kind of singularity for the stress components of isotropic domains involving a Voltra type screw dislocation. Faal et al. [15, 24] has reported Cauchy type singularity in orthotropic layers and four-sided domains weakened by a Voltra type screw dislocation.

3 THE ISOTROPIC WEDGE WITH AN ORTHOTROPIC COATING UNDER OUT OF PLANE DEFORMATION

In the current section, the analysis of the isotropic wedge with an orthotropic coating subjected to point traction τ_0 is studied (Fig. 1(b)). The Eq. (5) remain correct except that the first pair equations must be changed by

$$\tau_{\theta z}\left(r,0\right) = \tau_{\theta z}\left(r,\alpha\right) = \tau_0 \delta\left(r - r_0\right) \tag{21}$$

In which $\delta(\ldots)$ refers to the Dirac delta function. By making use of the boundary conditions (22) and applying Fourier transform to Eq. (3) gives

$$\begin{aligned} &r^2\frac{\partial^2 W\left(r,n\right)}{\partial r^2} + r\frac{\partial W\left(r,n\right)}{\partial r} - \left(Gn\kappa\right)^2 W\left(r,n\right) = 0, \quad R_1 \le r \le R_2 \\ &r^2\frac{\partial^2 W\left(r,n\right)}{\partial r^2} + r\frac{\partial W\left(r,n\right)}{\partial r} - \left(n\kappa\right)^2 W\left(r,n\right) = \frac{r\tau_0}{\mu_0}\left[1+\left(-1\right)^{n+1}\right]\delta\left(r-r_0\right), \quad R_2 \le r \le R_3 \end{aligned} \tag{22}$$

The solution of ordinary differential Eq. (22) can be written as:

$$\begin{cases} W\left(r,n\right)=C_1 r^{n\kappa}+D_1 r^{-n\kappa}, R_1\le r\le R_2 \\ W\left(r,n\right)=C_2 r^{Gn\kappa}+D_2 r^{-Gn\kappa}, R_2\le r\le r_0 \\ W\left(r,n\right)=C_3 r^{Gn\kappa}+D_3 r^{-Gn\kappa}, r_0\le r\le R_3 \end{cases} \tag{23}$$

The continuity of the stress components along the two sub-domains and the displacement components along the arcs $r=r_0$ and $r=R_2$ are stated as:

$$\begin{aligned} &W\left(r_0^-,n\right)=W\left(r_0^+,n\right) \\ &W\left(R_2^-,n\right)=W\left(R_2^+,n\right) \\ &G\frac{\partial}{\partial r}W\left(R_2^-,n\right)=\frac{\partial}{\partial r}W\left(R_2^+,n\right) \end{aligned} \tag{24}$$

By using the last pair Eq. (5) and by applying the continuity conditions of (24) to (23), we have

$$\begin{aligned} &C_1R_1^{n\kappa}+D_1R_1^{-n\kappa}=0 \\ &C_3R_3^{Gn\kappa}+D_3R_3^{-Gn\kappa}=0 \\ &C_3r_0^{Gn\kappa}+D_3r_0^{-Gn\kappa}=C_2r_0^{Gn\kappa}+D_2r_0^{-Gn\kappa} \\ &C_1R_2^{n\kappa}+D_1R_2^{-n\kappa}=C_2R_2^{Gn\kappa}+D_2R_2^{-Gn\kappa} \\ &C_1R_2^{n\kappa}-D_1R_2^{-n\kappa}=\bar{\mu}\left(C_2R_2^{Gn\kappa}-D_2R_2^{-Gn\kappa}\right) \end{aligned} \tag{25}$$

Eq. (22) is integrated along the arc $r=r_0$ as:

$$\int_{r_0^-}^{r_0^+}r^2\frac{\partial^2W\left(r,n\right)}{\partial r^2}dr+\int_{r_0^-}^{r_0^+}r\frac{\partial W\left(r,n\right)}{\partial r}dr-\left(n\kappa\right)^2\int_{r_0^-}^{r_0^+}W\left(r,n\right)dr=\frac{\tau_0}{G_2}\left[1+\left(-1\right)^{n+1}\right]\int_{r_0^-}^{r_0^+}r\delta\left(r-r_0\right)dr \tag{26}$$

Since the displacement components are continuous along the circular arcs $r=r_0$, Eq. (26) is simplified with the aid of the integration by-parts as:

$$\frac{\partial W\left(r_0^+,n\right)}{\partial r}-\frac{\partial W\left(r_0^-,n\right)}{\partial r}=\frac{\tau_0}{r_0\mu_0}\left[1+\left(-1\right)^{n+1}\right] \tag{27}$$

Using the Eqs. (28) and (24) gives

$$(C_3r_0^{Gn\kappa}-D_3r_0^{-Gn\kappa})-(C_2r_0^{Gn\kappa}-D_2r_0^{-Gn\kappa})=\frac{\tau_0}{n\kappa r_0\mu_0}\left[1+\left(-1\right)^{n+1}\right] \tag{28}$$

The unknown coefficients C_1, D_1, C_2 and D_2 are found by solving Eqs. (25) and (28). Upon substitution of the coefficients into Eq. (23), the displacement components can be obtained as:

$$\begin{aligned} &w\left(r,\theta\right)=\frac{2\tau_0}{\pi\bar{\mu}}\sum_{n=1}^{\infty}\Gamma_{\mathrm{n}}\left(1+\left(-1\right)^{n+1}\right)\left(1-\left(R_1/r\right)^{2n\kappa}\right)\left(r/r_0\right)^{n\kappa}\left(\left(r_0/R_3\right)^{2n\kappa}-1\right)\cos n\kappa\theta, \quad R_1\le r\le R_2 \\ &w\left(r,\theta\right)=\frac{\tau_0}{\pi\mu_0}\sum_{n=1}^{\infty}\Gamma_{\mathrm{n}}\left(r/r_0\right)^{Gn\kappa}\left(1+\left(-1\right)^{n+1}\right)\left(-1+\left(r_0/R_3\right)^{2Gn\kappa}\right)((\bar{\mu}+1)\left(-\left(R_1/r\right)^{2n\kappa}+1\right)-\left(\bar{\mu}-1\right) \end{aligned} \tag{29}$$

$$\left(-\left(R_2/r\right)^{2Gn\kappa}+\left(R_1/R_2\right)^{2Gn\kappa}\right))\cos n\kappa\theta,\quad R_2\le r\le r_0$$

$$w\left(r,\theta\right)=\frac{\tau_0}{\pi\mu_0}\sum_{n=1}^{\infty}\Gamma_{\mathrm{n}}\left(r_0/r\right)^{Gn\kappa}\left(1+\left(-1\right)^{n+1}\right)\left(-1+\left(r/R_3\right)^{2Gn\kappa}\right)((\bar{\mu}+1)\left(-\left(R_1/r_0\right)^{2Gn\kappa}+1\right)-(\bar{\mu}-1)$$

$$\left(-\left(R_2/r_0\right)^{2Gn\kappa}+\left(R_1/R_2\right)^{2Gn\kappa}\right))\cos n\kappa\theta,\quad r_0\le r\le R_3$$

In which $\Gamma_n=\dfrac{\Lambda_n}{\sin n\kappa\beta}$. With the aid of Eq. (2) stress filed in the entire domain can be obtained as:

$$\tau_{\theta z}\left(r,\theta\right)=-\frac{2\tau_0}{r\alpha}\sum_{n=1}^{\infty}n\left(1+\left(-1\right)^{n+1}\right)\Gamma_{\mathrm{n}}[-\left(r/r_0\right)^{Gn\kappa}+\left(rr_0/R_3^2\right)^{Gn\kappa}+\left(R_1^2/r_0r\right)^{Gn\kappa}$$

$$-\left(r_0R_1^2/rR_3^2\right)^{Gn\kappa}]\sin n\kappa\theta,\quad R_1\le r\le R_2$$

$$\tau_{\theta z}\left(r,\theta\right)=-\frac{\tau_0}{r\alpha}\sum_{n=1}^{\infty}n\left(1+\left(-1\right)^{n+1}\right)\Gamma_{\mathrm{n}}[(G+1)(-\left(r/r_0\right)^{Gn\kappa}+\left(rr_0/R_3^2\right)^{Gn\kappa}+\left(R_1^2/r_0r\right)^{n\kappa}$$

$$-\left(r_0R_1^2/rR_3^2\right)^{Gn\kappa})-(\bar{\mu}-1)(\left(rr_0R_1^2/R_2^2R_3^2\right)^{Gn\kappa}-\left(r_0R_1^2/rR_3^2\right)^{Gn\kappa}-\left(rR_1^2/r_0R_2^2\right)^{Gn\kappa}$$

$$+\left(R_2^2/r_0r\right)^{Gn\kappa})]\sin n\kappa\theta,\quad R_2\le r\le r_0$$

$$\tau_{\theta z}\left(r,\theta\right)=-\frac{\tau_0}{r\alpha}\sum_{n=1}^{\infty}n\Gamma_{\mathrm{n}}\left(1+\left(-1\right)^{n+1}\right)[(\bar{\mu}+1)(+\left(r_0/r\right)^{Gn\kappa}+\left(rr_0/R_3^2\right)^{Gn\kappa}+\left(R_2^2/r_0r\right)^{Gn\kappa}$$

$$+\left(r_0R_1^2/rR_3^2\right)^{Gn\kappa})-(\bar{\mu}-1)(\left(R_2^2/r_0r\right)^{Gn\kappa}+\left(rr_0R_1^2/R_2^2R_3^2\right)^{Gn\kappa}-\left(rR_2^2/r_0R_3^2\right)^{Gn\kappa}$$

$$-\left(r_0R_1^2/rR_2^2\right)^{Gn\kappa})]\sin n\kappa\theta,\quad r_0\le r\le R_3$$

$$\tau_{rz}\left(r,\theta\right)=\frac{2\tau_0}{r\alpha}\sum_{n=1}^{\infty}n\left(1+\left(-1\right)^{n+1}\right)\Gamma_{\mathrm{n}}[-\left(r/r_0\right)^{n\kappa}+\left(rr_0/R_3^2\right)^{n\kappa}-\left(R_1^2/r_0r\right)^{n\kappa}$$

$$+\left(r_0R_1^2/rR_3^2\right)^{n\kappa}]\cos n\kappa\theta,\quad R_1\le r\le R_2$$

$$\tau_{rz}\left(r,\theta\right)=\frac{\tau_0}{r\alpha}\sum_{n=1}^{\infty}n\left(1+\left(-1\right)^{n+1}\right)\Gamma_{\mathrm{n}}[(\bar{\mu}+1)\left(-\left(r/r_0\right)^{n\kappa}+\left(rr_0/R_3^2\right)^{n\kappa}-\left(R_1^2/r_0r\right)^{n\kappa}\right)$$

$$+\left(r_0R_1^2/rR_3^2\right)^{n\kappa}-(\bar{\mu}-1)\left(+\left(r_0R_1^2/rR_3^2\right)^{n\kappa}-\left(rR_1^2/r_0R_2^2\right)^{n\kappa}-\left(R_2^2/r_0r\right)^{n\kappa}\right)$$

$$+\left(rr_0R_1^2/R_2^2R_3^2\right)^{n\kappa}]\cos n\kappa\theta,\quad R_2\le r\le r_0$$

$$\tau_{rz}\left(r,\theta\right)=\frac{\tau_0}{r\alpha}\sum_{n=1}^{\infty}n\left(1+\left(-1\right)^{n+1}\right)\Gamma_{\mathrm{n}}[(\bar{\mu}+1)((r_0/r)^{Gn\kappa}+\left(rr_0/R_3^2\right)^{Gn\kappa}-\left(R_2^2/r_0r\right)^{Gn\kappa}$$

$$-\left(r_0R_1^2/rR_3^2\right)^{Gn\kappa})-(\bar{\mu}-1)\left(+\left(r_0R_1^2/rR_2^2\right)^{Gn\kappa}+\left(rr_0R_1^2/R_2^2R_3^2\right)^{Gn\kappa}-\left(R_2^2/r_0r\right)^{Gn\kappa}\right)$$

$$-\left(rR_2^2/r_0R_3^2\right)^{Gn\kappa}]\cos n\kappa\theta,\quad r_0\le r\le R_3$$

(30)

Similar to the dislocation solution, for sub-domain $r_0\le r\le R_3$, $\tau_{\theta z}\left(r,\theta\right)$ will be obtained by changing r/r_0 with r_0/r in the equation of $\tau_{\theta z}\left(r,\theta\right)$ for $R_2\le r\le r_0$. Similarly, for $\tau_{rz}\left(r,\theta\right)$ similar replacements must be

applied for each sub-domain. Furthermore, a minus sign is multiplied in the changed items. In addition, $n\Gamma_n$ must be replaced by $n\Lambda_n / \sin n\kappa\beta$. The stress filed can be summed up with the aid of the equation available in the reference [23].

$$
\begin{aligned}
&\tau_{\theta z}(r,\theta)=\frac{\tau_0}{r\alpha}\sum_{m=0}^{\infty}\sum_{l=0}^{m}\sum_{d=0}^{\infty}\Omega_{ld}^{m}\{[p_{ld}^{m}\left(rr_0/R_3^2,\theta\right)-p_{ld}^{m}\left(r_0R_1^2/rR_3^2,\theta\right)-p_{ld}^{m}\left(r/r_0,\theta\right)+p_{ld}^{m}\left(R_1^2/r_0r,\theta\right)]\\
&-[-p_{ld}^{m}\left(r/r_0,\alpha-\theta\right)+p_{ld}^{m}\left(rr_0/R_3^2,\alpha-\theta\right)-p_{ld}^{m}\left(r_0R_1^2/rR_3^2,\alpha-\theta\right)+q_{ld}^{m}\left(R_1^2/r_0r,\alpha-\theta\right)]\},\quad R_1\le r\le R_2\\
&\tau_{\theta z}(r,\theta)=\frac{\tau_0}{2r\alpha}\sum_{m=0}^{\infty}\sum_{l=0}^{m}\sum_{d=0}^{\infty}\Omega_{ld}^{m}\{(\bar{\mu}+1)(-p_{ld}^{m}\left(r/r_0,\theta\right)+p_{ld}^{m}\left(rr_0/R_3^2,\theta\right)-p_{ld}^{m}\left(r_0R_1^2/rR_3^2,\theta\right)\\
&+p_{ld}^{m}\left(R_1^2/r_0r,\theta\right)+p_{ld}^{m}\left(r/r_0,\alpha-\theta\right)-p_{ld}^{m}\left(rr_0/R_3^2,\alpha-\theta\right)-p_{ld}^{m}\left(R_1^2/r_0r,\alpha-\theta\right)\\
&+p_{ld}^{m}\left(r_0R_1^2/rR_3^2,\alpha-\theta\right))-(\bar{\mu}-1)(p_{ld}^{m}\left(rr_0R_1^2/R_2^2R_3^2,\theta\right)-p_{ld}^{m}\left(rR_1^2/r_0R_2^2,\theta\right)-p_{ld}^{m}\left(r_0R_1^2/rR_3^2,\theta\right)\\
&-p_{ld}^{m}\left(rr_0R_1^2/R_2^2R_3^2,\alpha-\theta\right)+p_{ld}^{m}\left(R_2^2/r_0r,\theta\right)+p_{ld}^{m}\left(r_0R_1^2/rR_3^2,\alpha-\theta\right)-p_{ld}^{m}\left(R_2^2/r_0r,\alpha-\theta\right)\\
&+p_{ld}^{m}\left(rR_1^2/r_0R_2^2,\alpha-\theta\right)),\quad R_2\le r\le r_0\\
&\tau_{rz}(r,\theta)=\frac{\tau_0}{r\alpha}\sum_{m=0}^{\infty}\sum_{l=0}^{m}\sum_{d=0}^{\infty}\Omega_{ld}^{m}\{[-q_{ld}^{m}\left(r/r_0,\theta\right)+q_{ld}^{m}\left(rr_0/R_3^2,\theta\right)+q_{ld}^{m}\left(r_0R_1^2/rR_3^2,\theta\right)-q_{ld}^{m}\left(R_1^2/r_0r,\theta\right)]\\
&-[-q_{ld}^{m}\left(r/r_0,\alpha-\theta\right)+q_{ld}^{m}\left(rr_0/R_3^2,\alpha-\theta\right)-q_{ld}^{m}\left(R_1^2/r_0r,\alpha-\theta\right)+q_{ld}^{m}\left(r_0R_1^2/rR_3^2,\alpha-\theta\right)]\},\quad R_1\le r\le R_2\\
&\tau_{rz}(r,\theta)=\frac{\tau_0}{2r\alpha}\sum_{m=0}^{\infty}\sum_{l=0}^{m}\sum_{d=0}^{\infty}\Omega_{ld}^{m}\{(\bar{\mu}+1)(q_{ld}^{m}\left(rr_0/R_3^2,\theta\right)+q_{ld}^{m}\left(r_0R_1^2/rR_3^2,\theta\right)-q_{ld}^{m}\left(r/r_0,\theta\right)\\
&-q_{ld}^{m}\left(rr_0/R_3^2,\alpha-\theta\right)-q_{ld}^{m}\left(R_1^2/r_0r,\theta\right)+q_{ld}^{m}\left(r/r_0,\alpha-\theta\right)\\
&-q_{ld}^{m}\left(r_0R_1^2/+q_{ld}^{m}\left(R_1^2/r_0r,\alpha-\theta\right)rR_3^2,\alpha-\theta\right))-(\bar{\mu}-1)(q_{ld}^{m}\left(rr_0R_1^2/R_2^2R_3^2,\theta\right)-q_{ld}^{m}\left(rR_1^2/r_0R_2^2,\theta\right)\\
&+q_{ld}^{m}\left(r_0R_1^2/rR_3^2,\theta\right)-q_{ld}^{m}\left(rr_0R_1^2/R_2^2R_3^2,\alpha-\theta\right)-q_{ld}^{m}\left(R_2^2/r_0r,\theta\right)+q_{ld}^{m}\left(rR_1^2/r_0R_2^2,\alpha-\theta\right)\\
&-q_{ld}^{m}\left(r_0R_1^2/rR_3^2,\alpha-\theta\right)+q_{ld}^{m}\left(R_2^2/r_0r,\alpha-\theta\right)),\quad R_2\le r\le r_0
\end{aligned}
\tag{31}
$$

It is to be noted that the stress and displacement components satisfy all of the continuity and boundary conditions of the problem. For $R_1=0$, Eq. (31) is simplified to available data in the reference [14], which shows the validity of the presented solution. We situate the local coordinate system (r',θ'), at the point load as $\theta=\sin^{-1}\left(r'sin\theta'/r\right),0\le\theta'\le\pi$ and $r=\sqrt{r'^2+r_0^2+2r'r_0cos\theta'}$, as shown in Fig. 1(b). By making use of these formulas, $(\tau_{rz},\tau_{\theta z})\sim 1/r'$ is deduced near the point load τ_0 that is, $r'\to 0$. This type of load singularity is available in elasticity books (see the reference [26]). By selecting a local coordinate in the wedge corners, we find that the stress filed does not show any singularity.

4 THE DISSIMILAR WEDGE UNDER TRACTION

In the current section, we use the dislocation solution presented in the previous section to analyze an isotropic wedge with an orthotropic coating weekend by multiple cracks and cavities with an arbitrary pattern. The elliptical cavities are assumed as non-singular closed-curve cracks [14, 15, 23, 24]. An isotropic coating wedge with an orthotropic coating containing M cavities, N_1 embedded cracks, and N_2 edge cracks which have been located at the isotropic wedge ($R_2\le r\le R_3$). Henceforth, we present the defects via the subscripts as:

$$
\begin{aligned}
&i \in \{1,2,\ldots,M\} \\
&j \in \{M+1, M+2,\ldots,M+N_1\} \\
&k \in \{M+N_1+1, M+N_1+2,\ldots,M+N_1+N_2\}
\end{aligned} \tag{32}
$$

In which $N = M + N_1 + N_2$ is the overall number of cracks and cavities. The out of plane stress component on the border of the *i-th* crack, $i = 1,2,\ldots,N$, in a cylindrical coordinate system can be written as:

$$
\begin{aligned}
\tau_{nz}(r_i,\theta_i) &= -\tau_{rz}(r_i,\theta_i)\sin\phi_i + \tau_{\theta z}(r_i,\theta_i)\cos\phi_i \\
\tau_{tz}(r_i,\theta_i) &= \tau_{rz}(r_i,\theta_i)\cos\phi_i + \tau_{\theta z}(r_i,\theta_i)\sin\phi_i
\end{aligned} \tag{33}
$$

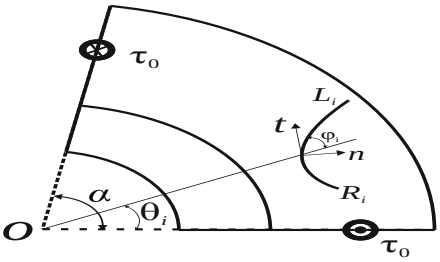

Fig.2
An isotropic wedge with an orthotropic coating containing a smooth crack.

In which ϕ_i refers to the angle between the tangential direction to the border of the *i-th* crack and the radial direction r_i. The dislocation solution or solution to Eq. (6) leads to the displacement component, which is also a solution to the governing equation of the problem, that is, Eq. (5). Also this solution with associated stress field (17) satisfies the equilibrium equation of the plane and the boundary condition of the domain. The governing equation and the boundary condition of the domain weakened by several defects are still Eqs. (4) and (13), respectively. Therefore, the dislocation solution is a solution for the crack problem satisfying the governing equation and the boundary conditions of a domain. There is a controlling parameter $b_z(S)$ which satisfies the boundary condition of the crack, that is, the crack surfaces must be traction free. It should be mentioned each crack has a specific b_z and this point causes to be considered interaction between the cracks. The screw dislocations with the density $B_{zj}(r_j)$ must be distributed along the segment at the border of the *j-th* crack. By making use of (32) and (17) the stress component on the border of the *i-th* crack corresponding to the dislocations is found as:

$$
\begin{aligned}
\tau_{nz}(r_i,\theta_i) = \frac{B_{jz}(r_j)G_2}{2r_i\alpha}[&\cos\phi_i \sum_{m=0}^{\infty}\sum_{l=0}^{m}\sum_{d=0}^{\infty}\Omega_{ld}^m \{q_{ld}^m\left(\frac{r_i r_j}{R_3^2},\theta_j-\theta_i\right)+q_{ld}^m\left(\frac{r_i}{r_j},\theta_j-\theta_i\right)-q_{ld}^m\left(\frac{r_j R_1^2}{r_i R_3^2},\theta_j-\theta_i\right) \\
&+q_{ld}^m\left(\frac{R_1^2}{r_i r_j},\theta_j+\theta_i\right)-q_{ld}^m\left(\frac{r_i r_j}{R_3^2},\theta_j+\theta_i\right)-q_{ld}^m\left(\frac{R_1^2}{r_i r_j},\theta_j-\theta_i\right)-q_{ld}^m\left(\frac{r_i}{r_j},\theta_j+\theta_i\right)+q_{ld}^m\left(\frac{r_j R_1^2}{r_i R_3^2},\theta_j+\theta_i\right)\} \\
&-\sin\phi_i \sum_{m=0}^{\infty}\sum_{l=0}^{m}\sum_{d=0}^{\infty}\Omega_{ld}^m \{p_{ld}^m\left(\frac{r_i r_j}{R_3^2},\theta_j-\theta_i\right)+p_{ld}^m\left(\frac{r_i}{r_j},\theta_j-\theta_i\right)+p_{ld}^m\left(\frac{r_j R_1^2}{r_i R_3^2},\theta_j-\theta_i\right)+p_{ld}^m\left(\frac{r_i r_j}{R_3^2},\theta_j+\theta_i\right) \\
&+p_{ld}^m\left(\frac{r_j R_1^2}{r_i R_3^2},\theta_j+\theta_i\right)+p_{ld}^m\left(\frac{R_1^2}{r_i r_j},\theta_j-\theta_i\right)+p_{ld}^m\left(\frac{R_1^2}{r_i r_j},\theta_j+\theta_i\right)+p_{ld}^m\left(\frac{r_i}{r_j},\theta_j+\theta_i\right)\}], \quad R_1 \le r_i \le R_2
\end{aligned} \tag{34}
$$

$$
\begin{aligned}
\tau_{nz}(r_i,\theta_i) = \frac{B_{jz}(r_j)G_2}{2r_i\alpha}\Bigg[&\cos\phi_i \sum_{m=0}^{\infty}\sum_{l=0}^{m}\sum_{d=0}^{\infty}\Omega_{ld}^m \{(\bar{\mu}+1)\Bigg[-q_{ld}^m\left(\frac{r_j R_1^2}{r_i R_3^2},\theta_j-\theta_i\right)+q_{ld}^m\left(\frac{r_i r_j}{R_3^2},\theta_j-\theta_i\right) \\
&+q_{ld}^m\left(\frac{r_i}{r_j},\theta_j-\theta_i\right)+q_{ld}^m\left(\frac{r_i r_j}{R_3^2},\theta_j+\theta_i\right)-q_{ld}^m\left(\frac{R_1^2}{r_i r_j},\theta_j-\theta_i\right)+q_{ld}^m\left(\frac{r_i}{r_j},\theta_j+\theta_i\right)-q_{ld}^m\left(\frac{r_j R_1^2}{r_i R_3^2},\theta_j+\theta_i\right)
\end{aligned}
$$

$$+q_{ld}^{m}\left(\frac{aR_1^2}{r_i R_3^2},\theta_j-\theta_i\right)-q_{ld}^{m}\left(\frac{r_i R_1^2}{aR_2^2},\theta_j-\theta_i\right)+q_{ld}^{m}\left(R_2^2/r_i a,\theta_j+\theta_i\right)-q_{ld}^{m}\left(\frac{R_2^2}{r_i r_j},\theta_j-\theta_i\right)+q_{ld}^{m}\left(\frac{r_i R_1^2}{r_j R_2^2},\theta_j-\theta_i\right)$$
$$+q_{ld}^{m}\left(\frac{r_i r_j R_1^2}{R_2^2 R_3^2},\theta_j-\theta_i\right)]-\sin\phi_i\sum_{m=0}^{\infty}\sum_{l=0}^{m}\sum_{d=0}^{\infty}\Omega_{ld}^{m}\{(\bar{\mu}+1)[+p_{ld}^{m}\left(\frac{r_j R_1^2}{r_i R_3^2},\theta_j-\theta_i\right)+p_{ld}^{m}\left(\frac{r_i r_j}{R_3^2},\theta_j-\theta_i\right)$$
$$+p_{ld}^{m}\left(\frac{r_i}{r_j},\theta_j-\theta_i\right)+p_{ld}^{m}\left(\frac{r_i r_j}{R_3^2},\theta_j+\theta_i\right)+p_{ld}^{m}\left(\frac{R_1^2}{r_i r_j},\theta_j-\theta_i\right)+p_{ld}^{m}\left(\frac{r_i}{r_j},\theta_j+\theta_i\right)+p_{ld}^{m}\left(\frac{r_j R_1^2}{r_i R_3^2},\theta_j+\theta_i\right)$$
$$+p_{ld}^{m}\left(\frac{R_1^2}{r_i r_j},\theta_j+\theta_i\right)]-(\bar{\mu}-1)[+p_{ld}^{m}\left(\frac{r_i r_j R_1^2}{R_2^2 R_3^2},\theta_j+\theta_i\right)+p_{ld}^{m}\left(\frac{r_j R_1^2}{r_i R_3^2},\theta_j+\theta_i\right)$$
$$+p_{ld}^{m}\left(\frac{R_2^2}{r_i r_j},\theta_j-\theta_i\right)+p_{ld}^{m}\left(\frac{r_i R_1^2}{r_j R_2^2},\theta_j-\theta_i\right)+p_{ld}^{m}\left(\frac{r_j R_1^2}{r_i R_3^2},\theta_j-\theta_i\right)+p_{ld}^{m}\left(\frac{r_i r_j R_1^2}{R_2^2 R_3^2},\theta_j-\theta_i\right)$$
$$+p_{ld}^{m}\left(\frac{R_2^2}{r_i r_j},\theta_j-\theta_i\right)+p_{ld}^{m}\left(\frac{r_i R_1^2}{r_j R_2^2},\theta_j-\theta_i\right)]],\quad R_2\le r_i\le r_j$$

The borders of cracks are covered by the screw dislocations and then stress component on the crack borders is achieved by making use of the theory of superposition. So, we integrate from Eq. (33) along the crack borders to be superimposed the ensuring tractions. Eq. (33) is integrated by describing the defects in parametric forms. For instance, an elliptical cavity with the minor and major semi-axes b_i and a_i (see the reference [14] for more details), can be described as follows:

$$\begin{aligned}
&r_i(s)=\{d_i{}^2+a_i{}^2b_i{}^2/[b_i{}^2\cos^2(\pi s+\omega_{si})+a_i{}^2\sin^2(\pi s+\omega_{si})]\\
&-2a_ib_id_i\cos(\pi s+\omega_{si}+\psi_{si})/\sqrt{b_i{}^2\cos^2(\pi s+\omega_{si})+a_i{}^2\sin^2(\pi s+\omega_{si})}\}^{\frac{1}{2}}\\
&\theta_i(s)=tan^{-1}\{d_i\sin\beta_i\sqrt{b_i{}^2\cos^2(\pi s+\omega_{si})+a_i{}^2\sin^2(\pi s+\omega_{si})}\\
&-a_ib_i\sin(\pi s+\omega_{si}+\psi_{si}+\beta_i)/[d_i\cos\beta_i\sqrt{b_i{}^2\cos^2(\pi s+\omega_{si})+a_i{}^2\sin^2(\pi s+\omega_{si})}\\
&-a_ib_i\cos(\pi s+\omega_{si}+\psi_{si}+\beta_i)]\}\\
&\phi_i(s)=tan^{-1}\left[r_i(s)\theta_i{}'(s)/r_i{}'(s)\right],\quad -1\le s\le 1
\end{aligned}\tag{35}$$

In which (d_i,β_i) is the center of the elliptical cavity. In addition, ω_{si} denotes the angle of the initial point and ψ_{si} refers to the angle of the major axis of the elliptical cavity. The prime sign describes a differentiation operation in Eq. (34). The stress component on the border of the *i-th* cack in the isotropic wedge reinforced by the orthotropic coating with N defects is written as:

$$\tau_{nz}\left(r_i(s),\theta_i(s)\right)=\sum_{j=1}^{N}\int_{-1}^{1}b_{zj}(t)k_{ij}(s,t)dt,\quad -1\le s\le 1,\quad i=1,2,\ldots,N \tag{36}$$

In which $b_{zj}(t)$ denotes the dislocation function on the normalized length of the *j-th* crack border. The kernel $k_{ij}(s,t)$ can be found in Appendix A. The newly defined functions $p_{00}^{0}\left(r_i(s)/r_j(t),\pi\left(\theta_j-\theta_i\right)/\alpha\right)$ and $q_{00}^{0}\left(r_i(s)/r_j(t),\pi\left(\theta_j-\theta_i\right)/\alpha\right)$ show singularity when we have $t\to s$. The external loading on the isotropic wedge with an orthotropic coating containing multiple cracks and cavities is Eq. (32). After multiplying a minus sign in the Eq. (31) and making use of Bueckner's attitude the left-side of Eq. (35) is the traction by the external

load on the intact isotropic wedge with an orthotropic coating wedge on the presumed defect border [27]. By making use of Eqs. (31) and (32), the resultant traction on the border of the *i-th* defect is achieved (Appendix B). By making use of the screw dislocation, the requirement equation for the crack opening along the *j-th* crack is written as:

$$w_j^+(s)-w_j^-(s)=\int_{-1}^{s}\sqrt{\left(r_j'(t)\right)^2+\left(r_j(t)\theta_j'(t)\right)^2}\,b_{zj}(t)dt\ ,\quad -1\le s\le 1,\quad j=1,2,\ldots,N \tag{37}$$

Note that the integral Eq. (36) must be solved under the following single-validness condition

$$\int_{-1}^{1}\sqrt{\left(r_j'(t)\right)^2+\left(r_j(t)\theta_j'(t)\right)^2}\,b_{zj}(t)dt=0,\quad j=1,2,\ldots,M+N_1 \tag{38}$$

The unknown dislocation densities on the borders of defects are calculated by evaluation of the integral Eqs. (36) and the single-validness condition (38) simultaneously. The solution of the integral Eqs. (36) is possible with a numerical method established by [14], Faal, Fariborz and Daghyani [15]. They proposed a numerical solution to reduce this kind of singular integral equations to a set of algebraic equations. The dislocation density function is written as a function of the weight function $g_{zj}(t)$ with the special feature that stresses at the crack tips must possess the traditional square-root singularity.

$$\begin{aligned} &b_{zj}(t)=\frac{g_{zj}(t)}{\sqrt{1-t^2}},\quad -1\le t\le 1 && \text{Embedded cracks}\\ &b_{zj}(t)=g_{zj}(t)\frac{\sqrt{1-t}}{\sqrt{1+t}},\quad -1\le t\le 1 && \text{Edge cracks}\end{aligned} \tag{39}$$

Since cavities are introduced as closed curved cracks without traditional singularities, the form of the dislocation density function in terms of the weight function is taken as:

$$b_{zj}(t)=g_{zj}(t)\sqrt{1-t^2},\quad -1\le t\le 1 \tag{40}$$

Stress intensity factors of the edge and embedded cracks are obtained as: [15]

$$\begin{cases} k_{IIILi}=\dfrac{\sqrt{\pi}}{2}\mu_0\left[\left(r_i'(-1)\right)^2+\left(r_i(-1)\theta_i'(-1)\right)^2\right]^{\frac{1}{4}}g_{zi}(-1) & \text{Embedded cracks}\\ k_{IIIRi}=-\dfrac{\sqrt{\pi}}{2}\mu_0\left[\left(r_i'(1)\right)^2+\left(r_i(1)\theta_i'(1)\right)^2\right]^{\frac{1}{4}}g_{zi}(1) & \\ k_{IIIi}=\sqrt{\pi}\mu_0\left[\left(r_i'(-1)\right)^2+\left(r_i(-1)\theta_i'(-1)\right)^2\right]^{\frac{1}{4}}g_{zi}(-1) & \text{Edge cracks}\end{cases} \tag{41}$$

As the strain on the defects is corresponding to the magnitude of dislocation density, the hoop stress on the border of the cavity is calculated as below

$$\tau_{tz}\left(r_i(s),\theta_i(s)\right)=\mu_0 b_{zi}(s),\quad -1\le s\le 1 \tag{42}$$

5 RESULTS AND DISCUSSION

In the current section, several numerical examples are presented to demonstrate the capability of the distributed dislocation technique in handling the problem involving different cases of cracks and cavities with arbitrary patterns.

Also we have used discrete points m = 60 in all examples. Since no publication has devoted to the out of plane deformation of a cracked wedge coated by an orthotropic layer, yet; the paper is validated with an isotropic infinite wedge without coating ($\bar{\mu}=1, R_1=0, R_2 \to R_3$ and $R_3 \to \infty$) containing two radial embedded cracks with equal lengths bisecting the apex angle is considered (see Fig.3). The distances between the center of each embedded crack and wedge apex are $d_1 = l/10$ and $d_2 = 3l/10$, in which the external loading is patch load on the two wedge borders with $l = 0.1m$. The graph of the normalized stress intensity factors k_{III}/k_0 , in which $k_0 = \tau_0\sqrt{\pi l}$, versus the length of the crack has been illustrated in Fig. 3. The normalized stress intensity factors obtained by the current method were in excellent agreement with the data illustrated in Fig. 4 of the work by Faal [23].

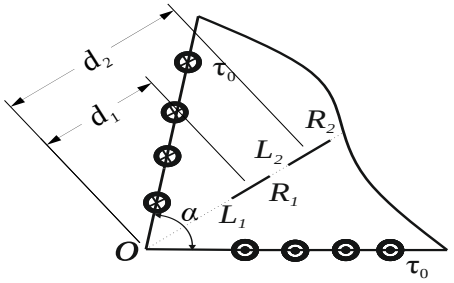

Fig.3
An infinite wedge weakened by two radial cracks.

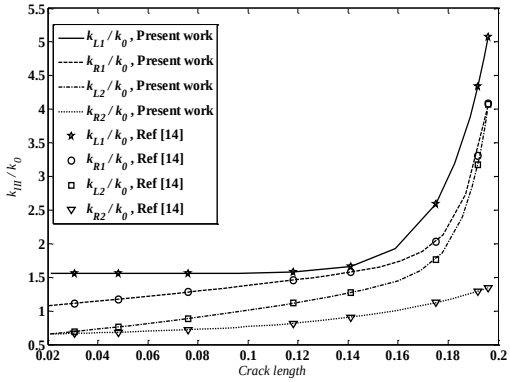

Fig.4
Normalized stress intensity factors for two embedded cracks against the normalized crack length.

In the following examples the dimensionless stress intensity factors are normalized to $k_0 = \tau_0\sqrt{\pi l}$. Also, l refers to the half-length of embedded cracks. The dimensionless hoop stresses are obtained by defining the dimensionless parameter τ_{tz}/τ_0 . In the following, the effect of the orthotropic coating layer is studied. We consider an isotropic wedge with $R_3 = 2R_1$ and the wedge angle is fixed at $\alpha = 2\pi/3$ for all examples. The external traction is a patch load with the magnitude of τ_0 distributed on the straight borders of the isotropic substrate. In the examples to follow, we calculate the dimensionless stress intensity factors , k_{III}/k_0 in which $k_0 = \tau_0\sqrt{\pi l}$. In addition, l is the half crack length. The effect of the orthotropic coating is studied by assuming $R_2 - R_1 = 0.1R_1$.

Example 1

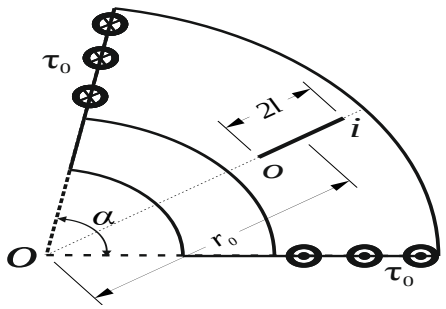

Fig.5
One radial embedded crack in an isotropic wedge with an orthotropic coating layer.

The first example of the problem is allocated to an isotropic wedge with an orthotropic coating weakened by one radial crack bisecting the apex angle, as shown in Fig.5. We set the center of the crack at the distance $r_0 = 1.6R_1$ from the origin of the domain under consideration. Variation of the normalized stress intensity factors versus the crack length, for two different orthotropic ratios is found in Fig.6. We can observe that the normalized stress intensity factors increases by the growth the crack length, but the crack tip *i* shows a little decrease with crack growth due to approaching the crack tip to the stress-free edge of the isotropic substrate. Also, Fig.6 displays changes of the orthotropic ratio from $G = 0.5$ to $G = 1.5$ and it can be observed the normalized stress intensity factors at the crack tips reduce with growth of the orthotropic ratio. In fact, a reduction in the normalized stress intensity factors occurs by making use of a suitable choice of the orthotropic ratio.

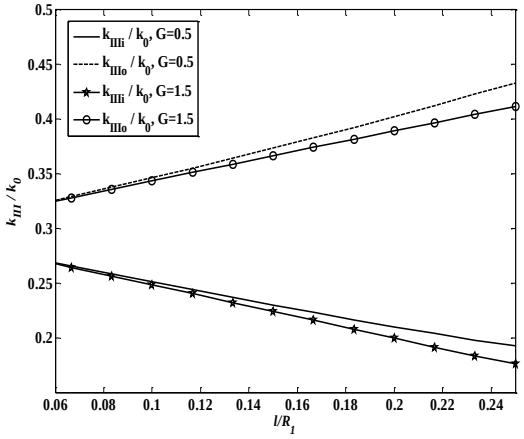

Fig.6
Variation of the normalized stress intensity factors against the normalized crack length.

In the following, the variation of normalized stress intensity factors against normalized orthotropic thickness, t/R_1, has been illustrated in Fig.7. The half-length of the crack is $l = 0.1R_1$. It is obvious that the increase of the orthotropic layer thickness reduces the normalized stress intensity factors.

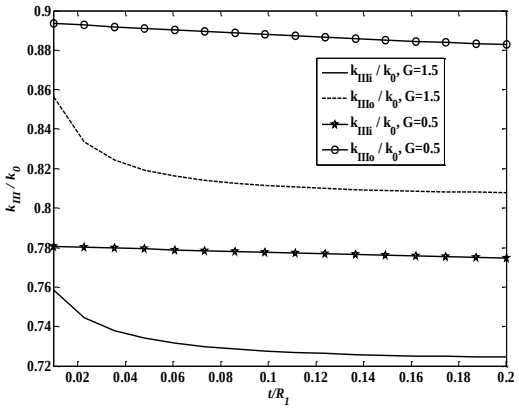

Fig.7
Variation of the normalized stress intensity factors against the normalized coating thickness.

Example 2

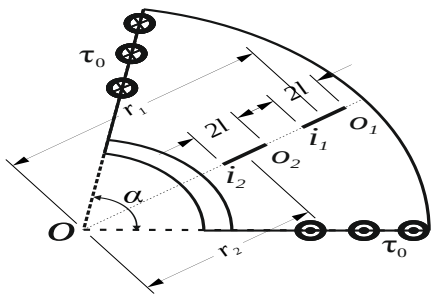

Fig.8
The domain weakened by two radial embedded cracks.

As the second example, two radial cracks with equal lengths bisecting the apex angle in an isotropic wedge with an orthotropic coating are considered (see Fig.8). The center of each crack is set at the distance $1.35R_1$ and $1.75R_1$ from the origin of the domain under consideration. Variation of the normalized stress intensity factors against the crack length has been illustrated in Fig.9. The normalized stress intensity factors for the crack tip i_1 and o_2 increase by the growth of the crack length because of the interaction between the crack tips. In general, we expected an increase of normalized stress intensity factors at the tip o_1 and i_2 by crack growth but a drop in the dimensionless stress intensity factors occurs due to receding from the crack tips i_1 and o_2. In the next graph of this example, the effect of the orthotropic layer thickness on the normalized stress intensity factors is studied. Therefore, the variation of the normalized stress intensity factors against the normalized orthotropic layer thickness for each crack tip can be realized in Fig.10, and the same trend of the previous example is obvious.

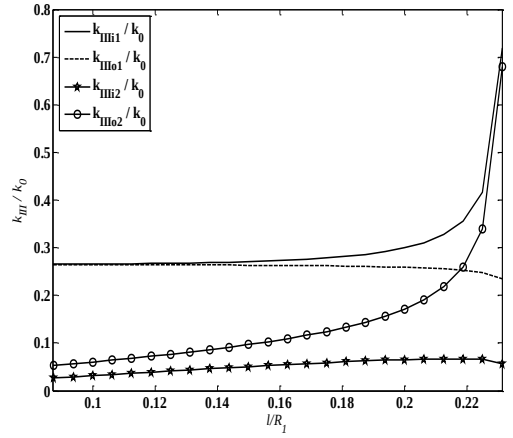

Fig.9
Variation of the normalized stress intensity factors against the normalized crack length for two embedded cracks ($G = 0.5$).

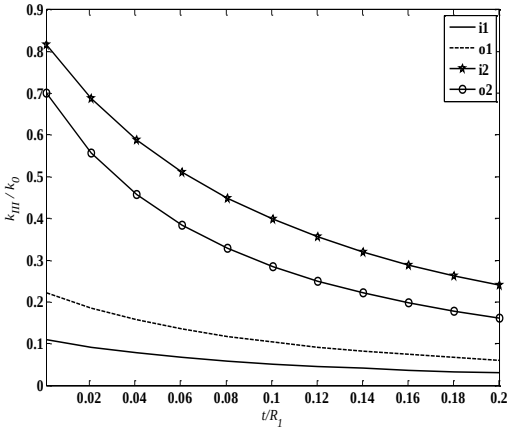

Fig.10
Variation of the normalized stress intensity factors against the normalized coating thickness for two embedded cracks ($G = 0.5$).

Example 3

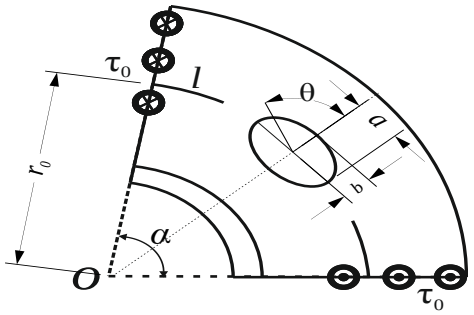

Fig.11
The domain under consideration containing one cavity and two circular edge cracks.

The interaction between two circular edge cracks and one cavity is studied for the next example. An isotropic substrate with an orthotropic layer weakened by one cavity with major and minor semi-axes $a = 0.4R_1$ and $b = 0.2R_1$ bisecting the apex angle and two symmetric circular edge cracks are considered (see Fig.11). The start point of each crack and the center of the cavity is placed at radius $r_0 = 1.6R_1$. Variation of the hoop stress around the elliptical cavity has been plotted in Fig.12, and it is obvious that the most value of the hoop stress occurs at the sharpest locations of the elliptical cavity. It is worth noting that these points are the closest points to the tips of the cracks. Next, the behavior of the normalized stress intensity factors against the normalized crack length is available for two orthotropic ratios in Fig.13. There is a minimum point in the profile of the stress intensity faction Fig.13. The normalized stress intensity factors go up as the lengths of the edge cracks become higher, but a decrease is observed because the crack tip is approaching to the elliptical cavity border with stress-free surface. Fig.14 shows the effect of the thickness ratio on the dimensionless stress intensity factors. It is to be noted that whatever the thickness of the coating increases, dimensionless stress intensity factors decrease more. Furthermore, the increase of the orthotropy ratio reduces the normalized stress intensity factors at the crack tips and the hoop stress around the cavity.

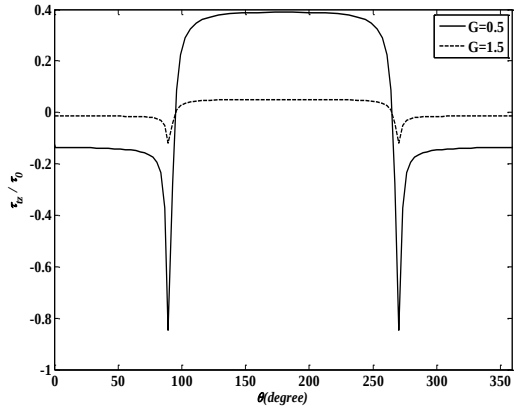

Fig.12
Variation of dimensionless hoop stresses around the elliptical cavity.

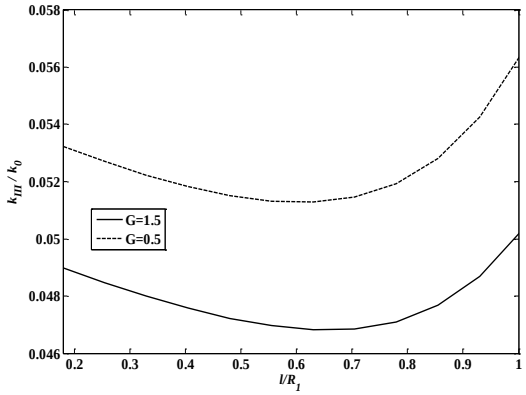

Fig.13
The graph of the normalized stress intensity factors against the normalized edge crack length.

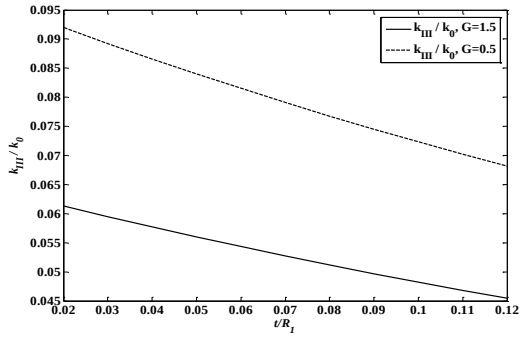

Fig.14
Variation of normalized stress intensity factors against the normalized orthotropic coating thickness.

Example 4

The last example to be investigated involves an isotropic wedge coated by an orthotropic layer weakened by two equal-sized cavities with major and minor semi-axes $a = 0.1R_1$ and $b = 0.05R_1$, respectively (see Fig.15). The centers of each cavity are considered to be at the distance $1.3R_1$ and $1.8R_1$ from the origin of the domain under consideration, respectively. Variations of the dimensionless hoop stresses on the surface of the cavities as a function of θ are depicted in Fig.16. It is obvious that the peaks of the dimensionless hoop stress on the surface of the cavities are found at the sharpest points of the defect.

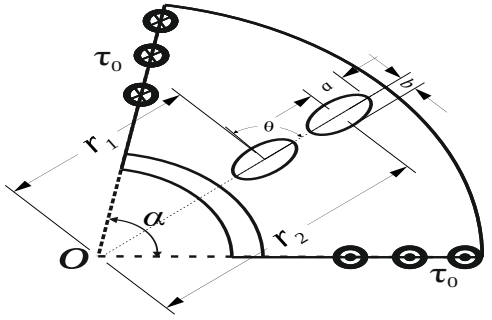

Fig.15
The domain under consideration weakened by two coaxial cavities.

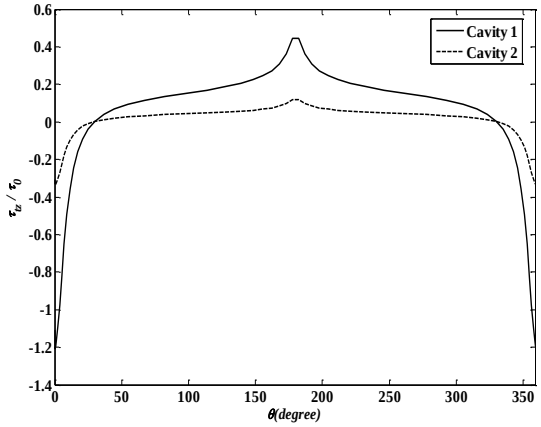

Fig.16
Variation of the normalized hoop stresses for the domain containing two cavities ($G = 0.5$).

6 CONCLUSION

In the present investigation, based on the LEFM theorem, an analytical solution was presented to calculate the stress intensity factors of the crack tips and the hoop stresses on the surface of the cavities in an isotropic wedge coated by an orthotropic layer subjected to out of plane deformation. At the first step, the stress components of an isotropic wedge coated by an orthotropic layer weakened by a screw dislocation were found in terms of the dislocation density function. To analyze the problem with several smooth cracks and cavities with an arbitrary pattern, the solution of the problem corresponding to the screw dislocation was simplified into a group of Cauchy integral equations by making use of the distributed dislocation approach. This kind of singular integral equation was solved numerically by reducing them to a set of algebraic equations. After evaluation of the integral equations, the stress intensity factors at the crack tips and hoop stresses around on the surface of the cavities was obtained. Briefly, Dimensionless stress intensity factor of crack tip is increased with crack grows but for an embedded some particular cracks there is a critical length which for crack length bigger than it, the dimensionless stress intensity factor is reduced. In other words, we see the crack growth is limited.

Future work will have to include different geometry of cross section and material, e.g., considering elliptical cross section and domains made of different material types such as FGMs.

APPENDIX

$$k_{ij}(s,t)=\frac{G_2}{2r_i(s)\alpha}[\cos\phi_i(s)\sum_{m=0}^{\infty}\sum_{l=0}^{m}\sum_{d=0}^{\infty}\Omega_{ld}^m\{-q_{ld}^m\left(\frac{r_j(t)R_1^2}{r_i(s)R_3^2},\theta_j(t)-\theta_i(s)\right)q_{ld}^m\left(\frac{r_i(s)r_j(t)}{R_3^2},\theta_j(t)-\theta_i(s)\right)$$
$$-q_{ld}^m\left(\frac{r_i(s)r_j(t)}{R_3^2},\theta_j(t)+\theta_i(s)\right)-q_{ld}^m\left(\frac{R_1^2}{r_i(s)r_j(t)},\theta_j(t)-\theta_i(s)\right)+q_{ld}^m\left(\frac{r_i(s)}{r_j(t)},\theta_j(t)-\theta_i(s)\right)$$
$$+q_{ld}^m\left(\frac{R_1^2}{r_i(s)r_j(t)},\theta_j(t)+\theta_i(s)\right)-q_{ld}^m\left(\frac{r_i(s)}{r_j(t)},\theta_j(t)+\theta_i(s)\right)+q_{ld}^m\left(\frac{r_j(t)R_1^2}{r_i(s)R_3^2},\theta_j(t)+\theta_i(s)\right)\}$$
$$-\sin\phi_i(s)\sum_{m=0}^{\infty}\sum_{l=0}^{m}\sum_{d=0}^{\infty}\Omega_{ld}^m\{p_{ld}^m\left(\frac{r_i(s)r_j(t)}{R_3^2},\theta_j(t)-\theta_i(s)\right)+p_{ld}^m\left(\frac{r_i(s)}{r_j(t)},\theta_j(t)-\theta_i(s)\right)+p_{ld}^m\left(\frac{r_j(t)R_1^2}{r_i(s)R_3^2},\theta_j(t)-\theta_i(s)\right)$$
$$+p_{ld}^m\left(\frac{R_1^2}{r_i(s)r_j(t)},\theta_j(t)+\theta_i(s)\right)+p_{ld}^m\left(\frac{r_i(s)}{r_j(t)},\theta_j(t)+\theta_i(s)\right)\}],\quad R_1\le r_i(s)\le R_2$$

$$k_{ij}(s,t)=\frac{G_2}{2r_i(s)\alpha}\Bigg[\cos\phi_i(s)\sum_{m=0}^{\infty}\sum_{l=0}^{m}\sum_{d=0}^{\infty}\Omega_{ld}^m\{(G+1)\Bigg[-q_{ld}^m\left(\frac{r_j(t)R_1^2}{r_i(s)R_3^2},\theta_j(t)-\theta_i(s)\right)+q_{ld}^m\left(\frac{r_i(s)r_j(t)}{R_3^2},\theta_j(t)-\theta_i(s)\right)$$
$$+q_{ld}^m\left(\frac{r_i(s)r_j(t)}{R_3^2},\theta_j(t)+\theta_i(s)\right)-q_{ld}^m\left(\frac{R_1^2}{r_i(s)r_j(t)},\theta_j(t)-\theta_i(s)\right)+q_{ld}^m\left(\frac{r_i(s)}{r_j(t)},\theta_j(t)-\theta_i(s)\right)$$
$$+q_{ld}^m\left(\frac{r_i(s)}{r_j(t)},\theta_j(t)+\theta_i(s)\right)-q_{ld}^m\left(\frac{r_j(t)R_1^2}{r_i(s)R_3^2},\theta_j(t)+\theta_i(s)\right)-q_{ld}^m\left(\frac{R_1^2}{r_i(s)r_j(t)},\theta_j(t)+\theta_i(s)\right)]$$
$$-(G-1)[-q_{ld}^m\left(\frac{r_i(s)r_j(t)R_1^2}{R_2^2R_3^2},\theta_j(t)+\theta_i(s)\right)+q_{ld}^m\left(\frac{r_j(t)R_1^2}{r_i(s)R_3^2},\theta_j(t)+\theta_i(s)\right)$$
$$+q_{ld}^m\left(\frac{R_2^2}{r_i(s)r_j(t)},\theta_j(t)+\theta_i(s)\right)+q_{ld}^m\left(\frac{r_j(t)R_1^2}{r_i(s)R_3^2},\theta_j(t)-\theta_i(s)\right)-q_{ld}^m\left(\frac{r_i(s)R_1^2}{r_j(t)R_2^2},\theta_j(t)-\theta_i(s)\right)$$
$$+q_{ld}^m\left(\frac{r_i(s)r_j(t)R_1^2}{R_2^2R_3^2},\theta_j(t)-\theta_i(s)\right)+q_{ld}^m\left(\frac{r_i(s)R_1^2}{r_j(t)R_2^2},\theta_j(t)-\theta_i(s)\right)]$$
$$-\sin\phi_i(s)\sum_{m=0}^{\infty}\sum_{l=0}^{m}\sum_{d=0}^{\infty}\Omega_{ld}^m\{(G+1)[p_{ld}^m\left(\frac{r_i(s)r_j(t)}{R_3^2},\theta_j(t)-\theta_i(s)\right)+p_{ld}^m\left(\frac{r_j(t)R_1^2}{r_i(s)R_3^2},\theta_j(t)-\theta_i(s)\right)$$
$$+p_{ld}^m\left(\frac{r_i(s)r_j(t)}{R_3^2},\theta_j(t)+\theta_i\right)+p_{ld}^m\left(\frac{R_1^2}{r_i(s)r_j(t)},\theta_j(t)-\theta_i(s)\right)+p_{ld}^m\left(\frac{r_i(s)}{r_j(t)},\theta_j(t)-\theta_i(s)\right)$$
$$+p_{ld}^m\left(\frac{r_i(s)}{r_j(t)},\theta_j(t)+\theta_i(s)\right)+p_{ld}^m\left(\frac{r_j(t)R_1^2}{r_i(s)R_3^2},\theta_j(t)+\theta_i(s)\right)+p_{ld}^m\left(\frac{R_1^2}{r_i(s)r_j(t)},\theta_j(t)+\theta_i(s)\right)]$$
$$-(G-1)[p_{ld}^m\left(\frac{r_j(t)R_1^2}{r_i(s)R_3^2},\theta_j(t)+\theta_i(s)\right)+p_{ld}^m\left(\frac{r_i(s)r_j(t)R_1^2}{R_2^2R_3^2},\theta_j(t)+\theta_i(s)\right)$$
$$+p_{ld}^m\left(\frac{R_2^2}{r_i(s)r_j(t)},\theta_j(t)+\theta_i(s)\right)+p_{ld}^m\left(\frac{r_j(t)R_1^2}{r_i(s)R_3^2},\theta_j(t)-\theta_i(s)\right)+p_{ld}^m\left(\frac{r_i(s)R_1^2}{r_j(t)R_2^2},\theta_j(t)-\theta_i(s)\right)$$
$$+p_{ld}^m\left(\frac{r_i(s)r_j(t)R_1^2}{R_2^2R_3^2},\theta_j(t)-\theta_i(s)\right)+p_{ld}^m\left(\frac{r_i(s)R_1^2}{r_j(t)R_2^2},\theta_j(t)-\theta_i(s)\right)+p_{ld}^m\left(\frac{R_2^2}{r_i(s)r_j(t)},\theta_j(t)-\theta_i(s)\right)]]],\quad R_2\le r_i(s)\le r_j(t)$$

$$\tau_{nz}\left(r_i,\theta_i\right)=\frac{\tau_0}{r_i\alpha}\{\sin\phi_i\sum_{m=0}^{\infty}\sum_{l=0}^{m}\sum_{d=0}^{\infty}\Omega_{ld}^{m}\{[q_{ld}^{m}\left(\frac{r_i r_0}{R_3^2},\theta_i\right)+q_{ld}^{m}\left(\frac{r_0R_1^2}{rR_3^2},\theta_i\right)-q_{ld}^{m}\left(\frac{r_i}{r_0},\theta_i\right)$$
$$-q_{ld}^{m}\left(\frac{R_1^2}{r_0r_i},\theta_i\right)]-[q_{ld}^{m}\left(\frac{r_i r_0}{R_3^2},\alpha-\theta_i\right)+q_{ld}^{m}\left(\frac{r_0R_1^2}{r_iR_3^2},\alpha-\theta_i\right)-q_{ld}^{m}\left(\frac{r_i}{r_0},\alpha-\theta_i\right)-q_{ld}^{m}\left(\frac{R_1^2}{r_0r_i},\alpha-\theta_i\right)]\}$$
$$-\cos\phi_i\sum_{m=0}^{\infty}\sum_{l=0}^{m}\sum_{d=0}^{\infty}\Omega_{ld}^{m}\{[p_{ld}^{m}\left(\frac{r_i r_0}{R_3^2},\theta_i\right)-p_{ld}^{m}\left(\frac{r_0R_1^2}{r_iR_3^2},\theta_i\right)-p_{ld}^{m}\left(\frac{r_i}{r_0},\theta_i\right)+p_{ld}^{m}\left(\frac{R_1^2}{r_0r_i},\theta_i\right)]$$
$$-[p_{ld}^{m}\left(\frac{r_i r_0}{R_3^2},\alpha-\theta_i\right)+q_{ld}^{m}\left(\frac{R_1^2}{r_0r_i},\alpha-\theta_i\right)-p_{ld}^{m}\left(\frac{r_i}{r_0},\alpha-\theta_i\right)-p_{ld}^{m}\left(\frac{r_0R_1^2}{r_iR_3^2},\alpha-\theta_i\right)]\}\},\quad R_1\le r_i\le R_2$$

$$\tau_{nz}\left(r_i,\theta_i\right)=\frac{\tau_0}{2r_i\alpha}\{\sin\phi_i\sum_{m=0}^{\infty}\sum_{l=0}^{m}\sum_{d=0}^{\infty}\Omega_{ld}^{m}\{(G+1)(q_{ld}^{m}\left(\frac{r_i r_0}{R_3^2},\theta_i\right)-q_{ld}^{m}\left(\frac{r_i}{r_0},\theta_i\right)-q_{ld}^{m}\left(\frac{R_1^2}{r_0r_i},\theta_i\right)$$
$$+q_{ld}^{m}\left(\frac{r_0R_1^2}{r_iR_3^2},\theta_i\right)+q_{ld}^{m}\left(\frac{r_i}{r_0},\alpha-\theta_i\right)-q_{ld}^{m}\left(\frac{r_i r_0}{R_3^2},\alpha-\theta_i\right)-q_{ld}^{m}\left(\frac{r_0R_1^2}{r_iR_3^2},\alpha-\theta_i\right)+q_{ld}^{m}\left(\frac{R_1^2}{r_0r_i},\alpha-\theta_i\right))$$
$$-(G-1)(q_{ld}^{m}\left(\frac{r_i r_0R_1^2}{R_2^2R_3^2},\theta_i\right)-q_{ld}^{m}\left(\frac{r_iR_1^2}{r_0R_2^2},\theta_i\right)+q_{ld}^{m}\left(\frac{r_0R_1^2}{r_iR_3^2},\theta_i\right)-q_{ld}^{m}\left(\frac{r_0r_iR_1^2}{R_2^2R_3^2},\alpha-\theta_i\right)-q_{ld}^{m}\left(\frac{R_2^2}{r_0r_i},\theta_i\right)$$
$$-q_{ld}^{m}\left(\frac{r_0R_1^2}{r_iR_3^2},\alpha-\theta_i\right)+q_{ld}^{m}\left(\frac{R_2^2}{r_0r_i},\alpha-\theta_i\right)+q_{ld}^{m}\left(\frac{r_iR_1^2}{r_0R_2^2},\alpha-\theta_i\right))-2\sum_{m=0}^{\infty}\sum_{l=0}^{m}\sum_{d=0}^{\infty}\Omega_{ld}^{m}$$
$$\{(G+1)(p_{ld}^{m}\left(\frac{r_i r_0}{R_3^2},\theta_i\right)-p_{ld}^{m}\left(\frac{r_i}{r_0},\theta_i\right)+p_{ld}^{m}\left(\frac{R_1^2}{r_0r_i},\theta_i\right)-p_{ld}^{m}\left(\frac{r_0R_1^2}{r_iR_3^2},\theta_i\right)+p_{ld}^{m}\left(\frac{r_i}{r_0},\alpha-\theta_i\right)-p_{ld}^{m}\left(\frac{r_i r_0}{R_3^2},\alpha-\theta_i\right)$$
$$-p_{ld}^{m}\left(\frac{R_1^2}{r_0r_i},\alpha-\theta_i\right)+p_{ld}^{m}\left(\frac{r_0R_1^2}{r_iR_3^2},\alpha-\theta_i\right))-(G-1)(p_{ld}^{m}\left(\frac{r_i r_0R_1^2}{R_2^2R_3^2},\theta_i\right)-p_{ld}^{m}\left(\frac{r_0R_1^2}{r_iR_3^2},\theta_i\right)+p_{ld}^{m}\left(\frac{R_2^2}{r_0r_i},\theta_i\right)$$
$$-p_{ld}^{m}\left(\frac{r_0r_iR_1^2}{R_2^2R_3^2},\alpha-\theta_i\right)-p_{ld}^{m}\left(\frac{r_iR_1^2}{r_0R_2^2},\theta\right)-p_{ld}^{m}\left(\frac{R_2^2}{r_0r_i},\alpha-\theta_i\right)+p_{ld}^{m}\left(\frac{r_0R_1^2}{r_iR_3^2},\alpha-\theta_i\right)+p_{ld}^{m}\left(\frac{r_iR_1^2}{r_0R_2^2},\alpha-\theta_i\right))\},\quad R_2\le r_i\le r_0$$

REFERENCES

[1] Erdogan F., 2000, Fracture mechanics, *International Journal of Solids and Structures* **37**: 171-183.

[2] Hills D.A., Kelly P., Dai D., Korsunsky A., 2013, *Solution of Crack Problems: The Distributed Dislocation Technique*, Springer Science & Business Media.

[3] Matbuly M., Nassar M., 2009, Analysis of multiple interfacial cracks in an orthotropic bi-material subjected to anti-plane shear loading, *Engineering Fracture Mechanics* **76**: 1658-1666.

[4] Li X-F., Duan X-Y., 2006, An interfacially-cracked orthotropic rectangular bi-material subjected to antiplane shear loading, *Applied Mathematics and Computation* **174**:1060-1079.

[5] Kargarnovin M., Fariborz S., 2000, Analysis of a dissimilar finite wedge under antiplane deformation, *Mechanics Research Communications* **27**:109-116.

[6] Kargarnovin M., Shahani A., Fariborz S., 1997, Analysis of an isotropic finite wedge under antiplane deformation, *International Journal of Solids and Structures* **34**:113-128.

[7] Shahani A., 1999, Analysis of an anisotropic finite wedge under antiplane deformation, *Journal of Elasticity* **56**:17-32.

[8] Shahani A., 2003, Mode III stress intensity factors for edge-cracked circular shafts, bonded wedges, bonded half planes and DCB's, *International Journal of Solids and Structures* **40**: 6567-6576.

[9] Lin R-L., Ma C-C., 2004, Theoretical full-field analysis of dissimilar isotropic composite annular wedges under anti-plane deformations, *International Journal of Solids and Structures* **41**: 6041-6080.

[10] Chen C-H., Wang C-L., 2009, A solution for an isotropic sector under anti-plane shear loadings, *International Journal of Solids and Structures* **46**: 2444-2452.

[11] Mkhitaryan S.M., Melkoumian N., Lin B.B., 2001, Stress-strain state of a cracked elastic wedge under anti-plane deformation with mixed boundary conditions on its faces, *International Journal of Fracture* **108**: 291-315.

[12] Shahani A., Ghadiri M., 2010, Analysis of anisotropic sector with a radial crack under anti-plane shear loading, *International Journal of Solids and Structures* **47**: 1030-1039.
[13] Lechnickij S.G., Lekhnitskiĭ S.G., 1963, *Theory of Elasticity of an Anisotropic Elastic Body*, Holden-Day.
[14] Faal R., Fariborz S., Daghyani H., 2007, Stress analysis of a finite wedge weakened by cavities, *International Journal of Mechanical Sciences* **49**: 75-85.
[15] Faal R.T., Fariborz S.J., Daghyani H.R., 2006, Antiplane deformation of orthotropic strips with multiple defects, *Journal of Mechanics of Materials and Structures* **1**: 1097-1114.
[16] Pook L.P., 2007, *Metal Fatigue What it is, Why it Matters*, Dordrecht, Springer.
[17] Pook L.P., 2003, A finite element analysis of cracked square plates and bars under antiplane loading, *Fatigue & Fracture of Engineering Materials & Structures* **26**: 533-541.
[18] Chen Y.Z., Lin X.Y., Chen R.S. 1997, Solution of torsion crack problem of an orthotropic rectangular bar by using computing compliance method, *Communications in Numerical Methods in Engineering* **13**: 655-663.
[19] Gracia L., Doblare M., 1988, Shape optimization of elastic orthotropic shafts under torsion by using boundary elements, *Computers & Structures* **30**: 1281-1291.
[20] Benveniste Y., Chen T., 2003, The Saint-Venant torsion of a circular bar consisting of a composite cylinder assemblage with cylindrically orthotropic constituents, *International Journal of Solids and Structures* **40**: 7093-7107.
[21] Rongqiao X., Jiansheng H., Weiqiu C., 2010, Saint-Venant torsion of orthotropic bars with inhomogeneous rectangular cross section, *Composite Structures* **92**: 1449-1457.
[22] Santoro R., 2010, The line element-less method analysis of orthotropic beam for the De Saint Venant torsion problem, *International Journal of Mechanical Sciences* **52**: 43-55.
[23] Faal R., Fotuhi A., Fariborz S., Daghyani H., 2004, Antiplane stress analysis of an isotropic wedge with multiple cracks, *International Journal of Solids and Structures* **41**: 4535-4550.
[24] Faal R., Daliri M., Milani A., 2011, Anti-Plane stress analysis of orthotropic rectangular planes weakened by multiple defects, *International Journal of Solids and Structures* **48**: 661-672.
[25] Weertman J., Weertman J., 1992, *Elementary Dislocation Theory*, Oxford University Press, New York.
[26] Barber J.R., 2002, *Elasticity*, Springer.
[27] Hills D.A., Kelly P.A., Dai D.N., Korsunsky A.M., 2013, *Solution of Crack Problems: The Distributed Dislocation Technique*, Springer Netherlands.